

27  
3-16-81  
JWS  
24 to NTHS

R-2727

①

UCID- 18909-Vol. I

**MASTER**

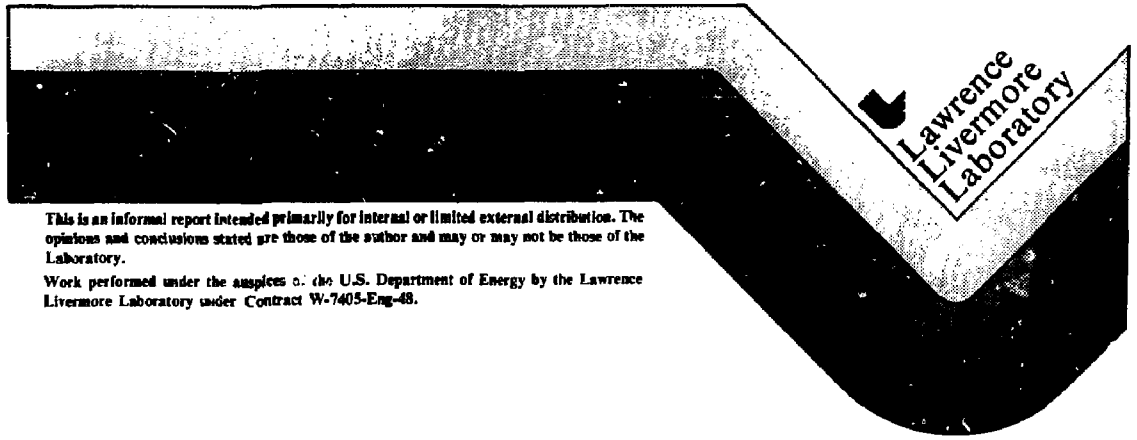
SYNFUELS FROM FUSION -  
PRODUCING HYDROGEN WITH THE  
TANDEM MIRROR REACTOR AND THERMOCHEMICAL CYCLES

R. W. Werner and F. L. Ribe  
Principal Investigators

R. Busch, B. C. Fryer, T. R. Galloway,  
M. R. Hoffman, O. H. Krikorian,  
D. S. Rowe and G. L. Woodruff  
Contributors

VOLUME I

January 21, 1981



This is an informal report intended primarily for internal or limited external distribution. The opinions and conclusions stated are those of the author and may or may not be those of the Laboratory.

Work performed under the auspices of the U.S. Department of Energy by the Lawrence Livermore Laboratory under Contract W-7405-Eng-48.

# SCOPING REPORT FY'80

SYNFUELS FROM FUSION —  
PRODUCING HYDROGEN WITH  
THE TANDEM MIRROR REACTOR  
AND THERMOCHEMICAL CYCLES

## PRINCIPAL INVESTIGATORS:

F.L. RIBE

DEPT. OF NUCLEAR ENGINEERING  
THE UNIVERSITY OF WASHINGTON  
SEATTLE, WASHINGTON 98195

R.W. WERNER

LAWRENCE LIVERMORE NATIONAL  
LABORATORY  
LIVERMORE, CALIFORNIA 94550

## WORK PERFORMED UNDER CONTRACTS:

FOR OFFICE OF FUSION ENERGY

DEPT. OF ENERGY

WASHINGTON DC 20545

W-740S-ENG 48LLNL

DE-AM06-76RL0222S

TA-DE AT06-76ET 52047- UNIVERSITY OF WASHINGTON

DISCLAIMER -



## TABLE OF CONTENTS

### VOLUME I

- Section A - A Brief Technical Summary
- Section 1 - Why Now for Synfuels
- Section 2 - Motivation for this Study
- Section 3 - Executive Summary

### VOLUME II

- Section 4 - The Tandem Mirror Fusion Driver
- Section 5 - The Cauldron Blanket Module
- Section 6 - The Flowing Microsphere
- Section 7 - Coupling the Reactor to the Process
- Section 8 - The Thermochemical Cycles
- Section 9 - Chemical Reactors and Process Units

SECTION A  
A BRIEF TECHNICAL SUMMARY

This report examines, for technical merit, the combination of a fusion reactor driver and a thermochemical plant as a means for producing synthetic fuel in the basic form of hydrogen.

We studied:

- One reactor type--the Tandem Mirror Reactor--wishing to use to advantage its simple central cell geometry and its direct electrical output.
- Two reactor blanket module types--a liquid metal cauldron design and a flowing  $\text{Li}_2\text{O}$  solid microsphere pellet design so as to compare the technology, the thermal-hydraulics, neutronics and tritium control in a high-temperature operating mode (~1200 K).
- Three thermochemical cycles--processes in which water is used as a feedstock along with a high-temperature heat source to produce  $\text{H}_2$  and  $\text{O}_2$ . The water splitting process is a closed loop sequence of chemical reactions in which the reagents ( $\text{H}_2\text{SO}_4$ , I and Br in the cases studied) are continuously recycled. The cycles are: the General Atomic Sulfur-Iodine; the Westinghouse Sulfur; and the Ispra, Italy, Sulfur Bromine cycles. Only these three cycles, of approximately 30 studied world-wide, have been developed to laboratory model levels and produced demonstration quantities of hydrogen.

## Major Conclusions

- We are satisfied that the production of hydrogen using thermochemical cycles has a demonstrated experimental base and potential for commercial exploration.
- There are only three drivers for the processes:
  - (a) the fusion reactor
  - (b) the HTGR or VHTR
  - (c) solar
- As drivers the fusion reactor and the HTGR have an edge over solar because the thermochemical cycle cannot be interrupted by diurnal effects.
- Generic fusion reactors and the HTGR are both good candidates for synfuel drivers.
- By fusion reactor type, the TMR has an advantage over the Tokamak, both topologically and due to energy output form.
- The TMR confinement physics for synfuels is substantially the same as it would be for electrical production.
- The key problem in the reactor is designing a high-temperature (1200 K) blanket module.
  - Particle sintering, extreme temperatures in the zone dividers and complicated heat transfer preclude the use of the  $\text{Li}_2\text{O}$  pellet design.

- The cauldron pool boiler design fares quite well structurally, mechanically, neutronically, for assembly/disassembly, for isolation, for safety by modularization, for low residual activity, as a low stress structure and as a good module for low tritium inventories and integral tritium production. It requires experimental verification of MHD effects and energy transfer within the pool.
- For either blanket design the quantity of process heat delivered to the chemical plant at 1200 K was excellent, ~90%.
- Materials problems at 1200 K and in corrosive atmospheres are difficult. However, we are encouraged in having found a set of contemporary materials believed adequate for the temperature/environment situations.
- We believe we have introduced an improved design for the SO<sub>3</sub> decomposer--the most difficult unit in the chemical plant--by using a fluidized bed process rather than the packed bed used heretofore.

#### Conclusion and Recommendations

We conclude that the Fission/Synfuel tie is a good one with a high eventual payoff. The problems are difficult but the study is in its infancy. Even during this short study period, we have begun to resolve some of the problems and see possible solutions for others. The program needs and deserves support.

We recommend this follow-on work:

1. Exploration of an alternative to the basic cauldron blanket module--the cauldron with heat pipes.
2. The use of surplus dc and thermal energy from the direct convertor (at  $Q > 11$ ) to joule heat the process fluid driving the  $SO_3$  decomposer. This may allow relaxation of blanket temperatures and transport piping temperatures by several hundred degrees. It also allows reconsideration of the solid  $Li_2O$  blanket.

These two major steps can serve to decrease materials temperature requirements of the blanket, isolate the high temperatures to the  $SO_3$  decomposer unit and decrease the process chemistry complexity of the sulphuric acid section of the process.

SECTION 1  
WHY NOW FOR FUSION AND SYNFUELS

Compiler: R. Werner

<u>Section</u>	<u>Description</u>	<u>Page</u>
1.1	Introduction . . . . .	1-2
1.2	Changes in U.S. Energy Posture . . . . .	1-3
1.3	Fusion and the National Energy Plan . . . . .	1-4
1.4	Energy Areas Where Fusion Can Impact . . . . .	1-4

LIST OF FIGURES

<u>Figure</u>	<u>Title</u>	<u>Page</u>
1.1	U.S. Energy Flow - 1979 . . . . .	1-5
1.2	U.S. Energy Flow - 2000 . . . . .	1-6

1.0 WHY NOW FOR FUSION AND SYNFUELS

1.1 Introduction

The research and development program for controlled nuclear fusion has from the beginning been directed toward central station electrical power plants as the ultimate application. The original basis for this choice was sound and rested on several assumptions regarding the various alternative forms of energy in the U.S.

The most important assumptions regarding electricity were the following:

a. Cost

Electricity has been the most expensive of the large-scale forms of energy in the U.S. It therefore offered a promising market for new energy technologies.

b. Growth Rate

For many years the annual growth in the production and consumption of electricity in the U.S. was approximately 7 percent. This is a high rate of growth, and it has long been clear that important new sources of electrical power would have to be developed in order to maintain such a rate for the long term.

c. Central Station Compatibility

There are important economies of scale associated with large central station electrical power plants, and electrical utilities have both distribution grids and operational systems which incorporate such plants. Most of the magnetic fusion confinement concepts tend to be

large, at least comparable in size to plants now being built; therefore, they are compatible with the central station plant theme.

The alternative energies which are relevant to this discussion are those derived from fluid fuels, oil, and natural gas. The more important assumptions about them were complementary to those regarding electrical energy. Until very recently, these portable fuels have, for a variety of reasons, been comparatively inexpensive in the U.S. Similarly, availability was not an issue, at least in the minds of most people. The U.S. was an exporter of oil until the mid-1960's. Finally, there were serious technical questions regarding the feasibility of synthetic production of fluid fuels.

1.2

#### Changes in U.S. Energy Posture

Dramatic changes in the U.S. energy posture have occurred in the last few years. Some of these changes may have a large and direct impact on the potential applications of fusion energy. The U.S. is now heavily dependent (about 50%) upon imports for oil. These imports come at rapidly increasing prices and to a great extent from politically unstable regions. Furthermore, these imports are required, to a large extent, to satisfy the increasing demand for portable fuels in the transportation, industrial, residential, and commercial areas, while the demand for electricity has leveled off with a growth rate lower than our economic growth. Our average national generating capacity is adequate. There may remain local shortages of electrical generating capacity, but becoming more dominant is the need for fuel to drive them. It is evident that the U.S. must have domestic sources of energy, both to fuel our electrical plants and to respond to our other areas of energy flow.

### 1.3 Fusion and the National Energy Plan

The nation has finally started on a national energy plan and a substantial synthetic fuel program. Studies on fusion reactors for synfuel production should become part of this energy plan and part of the synfuel venture now, not later, even though our reactor may be 20 or 25 years in the future. It is time to actively include synthetic fuel production in the fusion program.

### 1.4 Energy Areas Where Fusion Can Impact

The flow of the various forms of energy in the U.S. for 1979 is given in Fig. 1.1. A similar set of data predicted for the year 2000 is shown in Fig. 1.2. The areas where we believe fusion/synfuel can impact are shown in black. It is instructive to compare the magnitude of this potential application with that involving only electricity. In terms of end-use, the potential market for synfuel is greater than that for electricity by approximately a factor of 5. In terms of total production, the ratio is a factor of about 3.

The background for the fusion/synfuel study being undertaken by this project can thus be simply stated. Can fusion reactor technology be made to be compatible with the economically competitive production of synthetic fuel? If the answer to this question is in the affirmative, then the potential market for fusion power is increased by a substantial factor, perhaps 200 percent. Furthermore, by producing a direct substitute for a more strategic form of energy, the potential contribution of fusion to the national interest could be multiplied by an even greater factor.

The progress reported here is of a study of the above question by a project team consisting of personnel from Lawrence Livermore National Laboratory, the University of Washington, and Exxon Nuclear Co., Inc.

**U.S. ENERGY FLOW - 1979**  
**(NET PRIMARY RESOURCE CONSUMPTION 77.8 QUADS)**

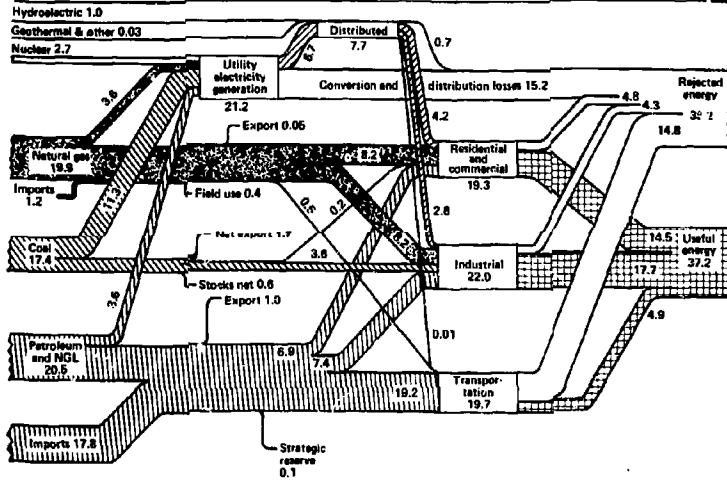


Fig. 1.1 U.S. Energy Flow - 1979

# U.S. ENERGY FLOW-2000



SRI ENERGY MODEL- LLL NOMINAL  
(PRIMARY RESOURCE CONSUMPTION 157.5 QUADS)

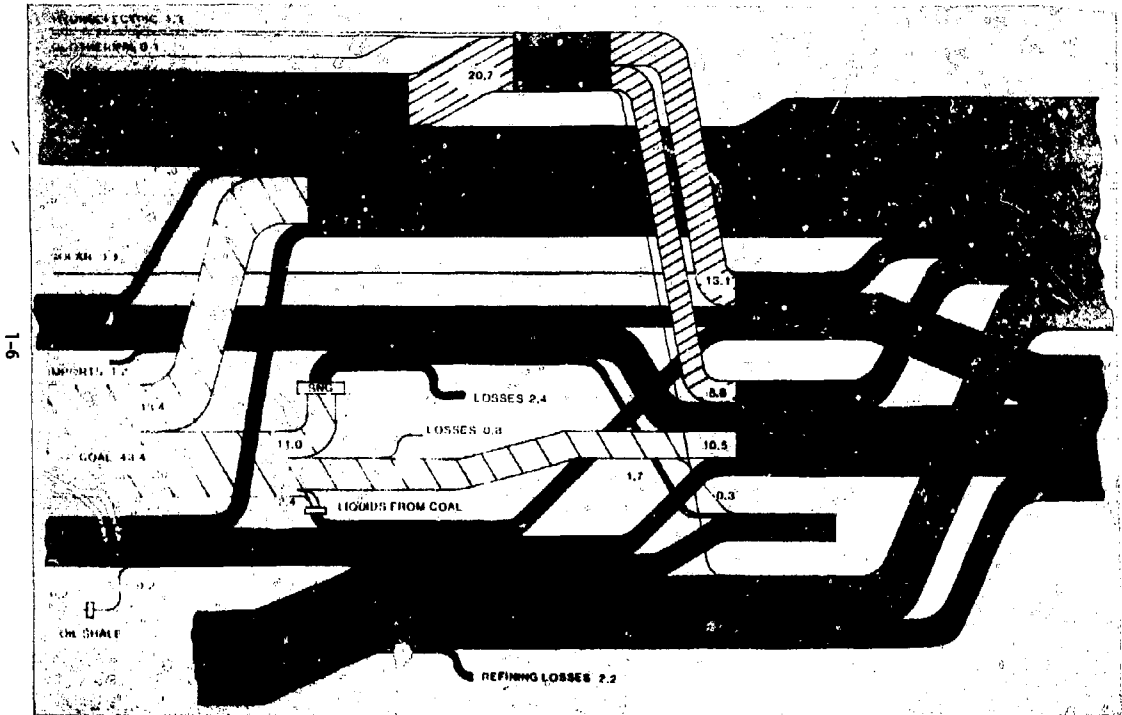


Fig. 1.2 U.S. Energy Flow - 2000

SECTION 2  
STUDY METHOD AND ORGANIZATION

Compiler: R. Werner

<u>Section</u>	<u>Description</u>	<u>Page</u>
2.1	Technical Approach . . . . .	2-2
2.2	Organization . . . . .	2-4

LIST OF FIGURES

<u>Figure</u>	<u>Title</u>	<u>Page</u>
2.1	Fusion-Based Hydrogen Production System . . . . .	2-3
2.2	Organizational Setup . . . . .	2-6

## 2.0 STUDY METHOD AND ORGANIZATION

### 2.1 Technical Approach

The project team has defined four major plant components that must be designed and interfaced in a self-consistent manner to constitute a total fusion/synfuel plant. As shown in Fig. 2.1, these components are: (1) the Tandem Mirror Reactor (TMR), with its associated physics; (2) the reactor blanket/shield and direct convertor, source of the process energy; (3) the energy transport and conversion system; and (4) the synfuel plant, producer of the hydrogen fuel.

In order to perform reasonably detailed technical analyses, it has been necessary to select specific types of components. Insofar as possible, the options which are most attractive and suitable for the overall design have been identified. Whether or not the choices made are indeed optimal in every case, it is reasonable to expect that the major problem areas can be identified and meaningful feasibility assessments performed. Furthermore, much of the work related to the fusion driver--reactor physics, the blanket, the direct convertor, the energy transport and conversion system--is also directly relevant to the development of fusion reactor technology for electrical production.

The specific types of components selected for the study, after preliminary screening, were the following:

- (1) Fusion Driver--Tandem Mirror Reactor
- (2) Reactor Blanket--two different types: (a) a Li-Na cauldron and (b) a flowing  $\text{Li}_2\text{O}$  microsphere design
- (3) Transport and Conversion System--five different options: (a) single series sodium, (b) helium series/

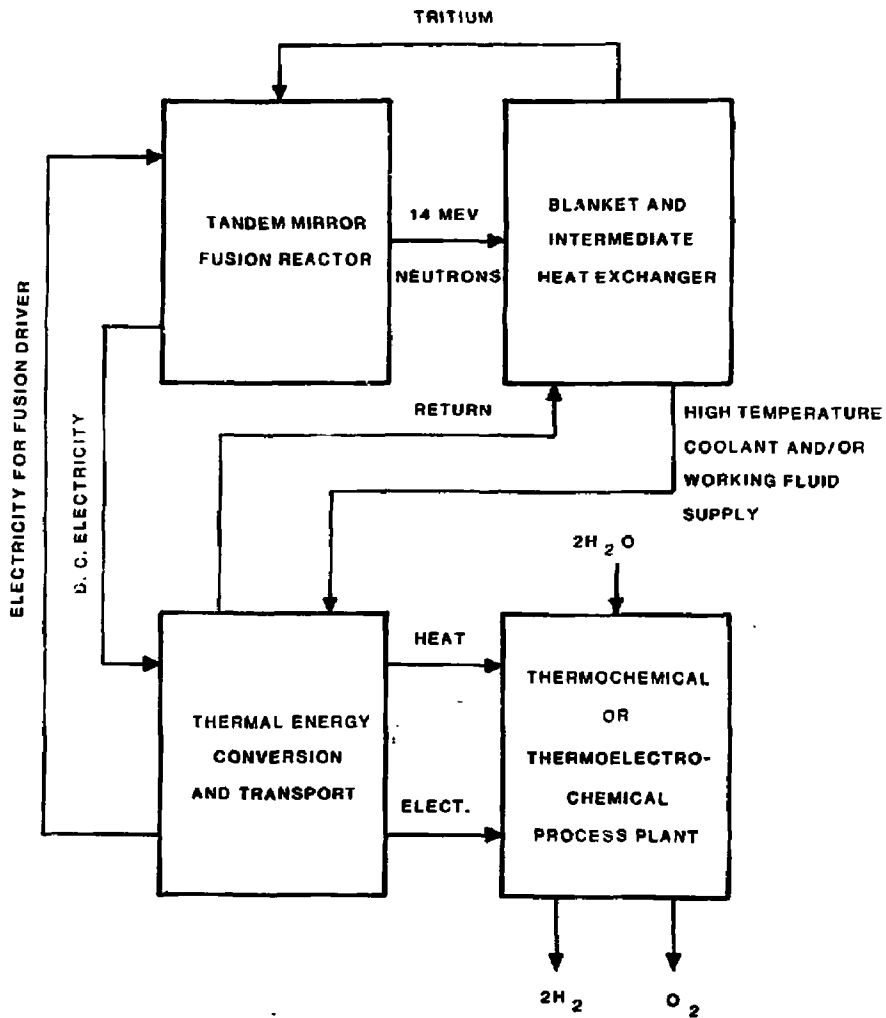


Fig. 2.1 Fusion-Based Hydrogen Production System

parallel, (c) potassium series/parallel, (d) potassium parallel, and (e) sodium with hydrogen recycle

- (4) Synfuel Plant--the General Atomic Sulfur Iodine Cycle for hydrogen production. The Ispra Sulphur Bromine Cycle provides a backup.

## 2.2 Organization

The project was conducted by personnel from the Lawrence Livermore National Laboratory, the University of Washington, and Exxon Nuclear Company, Inc. The individuals involved represented several different complementary scientific and engineering disciplines. Assignments were made for specific areas, with subsequent critiques and interfacing efforts performed by the entire group. In general, the plan was organized as follows to produce the scoping design described in this report.

The Lawrence Livermore National Laboratory provided:

-Management and Coordination	R. Werner, jointly with F. Ribe, UW
-Fusion Reactor Physics	Staff
-Fusion Engineering/Technology	R. Werner/M.Hoffman*
-Physical Chemistry/Materials	O. Krikorian
-Chemical Process Engineering and Design	T. Galloway
-Cauldron Module Design	R. Werner
-Transport System	T. Galloway/R. Werner
-Thermal Hydraulics	R. Werner

\*Professor, Mechanical Engineering, UC Davis

University of Washington provided:

-Physics	F. Ribe/Students
-Computer Sciences	K. Audenaerde
-Neutronics	G. Woodruff/Students
-Energy Balance	F. Ribe/Students

Exxon provided:

-Chem Process Engineering	B. Fryer
-Thermal Hydraulics	D. Rowe (of Rowe and Associates, subcontractor to Exxon)
-Flowing Microsphere Module Design	D. Rowe
-Li <sub>2</sub> O Mech/Chem Properties	R. Busch

This organizational setup is shown in Figure 2.2.

THE COOPERATIVE

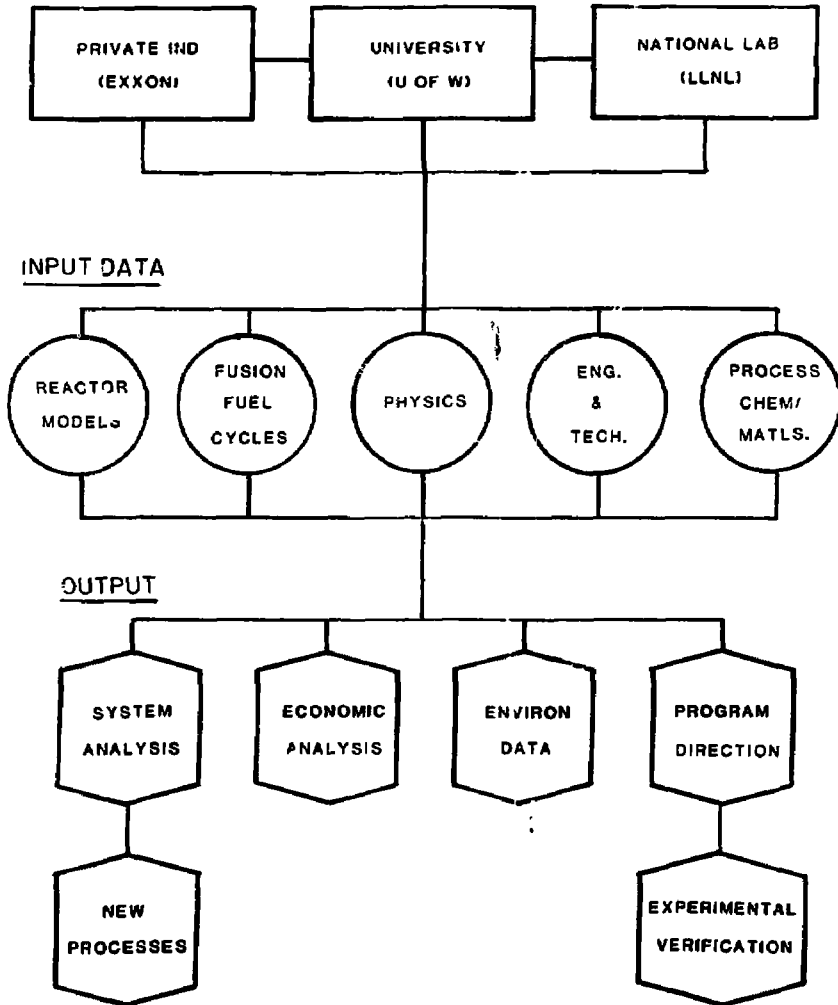


Fig. 2.2 Organizational Setup

SECTION 3

EXECUTIVE SUMMARY

Compiler: R. Werner

<u>Section</u>	<u>Description</u>	<u>Page</u>
3.1	Summary of our Findings . . . . .	3-6
3.2	The Technical Choice of the TMR . . . . .	3-11
3.2.1	The Confinement Physics . . . . .	3-12
3.2.2	The Reactor Topology . . . . .	3-14
3.3	The Tandem Mirror Reactor Energy Forms . . . . .	3-14
3.4	The Energy Needs of the Thermochemical Cycles . . . . .	3-18
3.5	The Tandem Mirror Reactor Energy Balance, Thermal and Electric . . . . .	3-20
3.6	The Influence of Q on the TMR's Uniqueness . . . . .	3-21
3.7	Conclusions on the Tandem as an Energy Source . . . . .	3-25
3.8	TMR Design Parameters - Thermochemical Hydrogen vs Electrical Production . . . . .	3-26
3.9	Synfuel Influence on Reactor Design . . . . .	3-26
3.10	The Reactor Blanket Designs . . . . .	3-27
3.10.1	Operating Principle of the Cauldron Blanket Module . . . . .	3-27
3.10.2	Materials Selections for the Cauldron . . . . .	3-30
3.10.3	Conclusions and Observations on the Cauldron . . . . .	3-34
3.10.4	Flowing Microsphere Blanket and Module Heat Exchanger . . . . .	3-38
3.11	Heat Transport System Reactor to Thermochemical Process . . . . .	3-44
3.12	Thermochemical Plant Process . . . . .	3-46

<u>Section</u>	<u>Description</u>	<u>Page</u>
3.12.1	Basic Principles of Thermochemical Cycles . . . . .	3-46
3.12.2	Chemical Description of the General Atomic Cycle . . . . .	3-47
3.12.3	The Fluidized Bed SO <sub>3</sub> Decomposer . . . . .	3-48
3.12.4	A Fluidized Bed SO <sub>3</sub> Decomposer Design . . . . .	3-51
3.13	Process Chemistry Structural Materials . . . . .	3-54
3.14	Coupling the Fusion Reactor to the Thermochemical Hydrogen Production Process . . . . .	3-56
3.15	Integrated TMR-Synfuel Plant Energy Balance . . . . .	3-65
3.16	Looking to the Future - The TMR and the D-D or D-He Cycle .	3-68

### SECTION 3

#### LIST OF FIGURES

<u>Figure</u>	<u>Title</u>	<u>Page</u>
3.1	TMR with Thermal Barriers . . . . .	3-11
3.2	Axial Magnetic Field and Electrostatic Profiles in the TMR with Thermal Barriers . . . . .	3-13
3.3 A, B, C, D, E	Assembly of Blanket Modules . . . . .	3-15
3.4	The Tandem Mirror Reactor Energy Source Compared with Other Energy Sources . . . . .	3-22
3.5	TMR Energy Balance . . . . .	3-23
3.6	Units of Surplus Electrical Energy vs Q for the TMR . . . .	3-24
3.7	Net dc Power Available to the Process Plant as a Percentage of Total Process Heat . . . . .	3-24
3.8 A & B	Cross Section and Isometric Views of the Cauldron Blanket Module . . . . .	3-28
3.9	Schematic Description of a Ten Zone Flow Microsphere Baffled Blanket . . . . .	3-39
3.10	Flowing Li <sub>2</sub> O Blanket Concept Schematic for Thermochemical Hydrogen Production . . . . .	3-40
3.11	Exit Temperature Distribution from Ten Zone Blanket . . . .	3-41
3.12	Illustration of Temperature Distributions through Uncooled Baffle Sections . . . . .	3-43
3.13	Hydrogen Production by Decomposition of 96% H <sub>2</sub> SO <sub>4</sub> . . . .	3-49
3.14	Fluidized bed catalytic SO <sub>3</sub> Decomposer . . . . .	3-52
3.15	Fusion Based Hydrogen Production System . . . . .	3-57
3.16	Single Series Na Loop-Electric Power Generation Based on LMFBR Technology Subsystem A . . . . .	3-59
3.17	Combined Series/Parallel Subsystem Utilizing Helium as the Thermal Transport Media and Working Fluid for Generating Most of the Required Electricity . . . . .	3-62

<u>Figure</u>	<u>Title</u>	<u>Page</u>
3.18	Combined Series/Parallel Subsystem Utilizing K as the Working Fluid . . . . .	3-63
3.19	Power Flow Diagram for the TMR-Synfuel System with Bottoming Electric Power Generation . . . . .	3-66
3.20	Power Flow Diagram for the TMR-Synfuel System with Topping and Bottoming Electric Power Generation . . . . .	3-67
3.21	Gross Fusion Power and External Recirculating Power as Functions of Fusion Reactor Gain Q . . . . .	3-69
3.22	Overall Efficiency Potential of Different Energy Sources . . . . .	3-70

SECTION 3  
LIST OF TABLES

<u>Table</u>	<u>Title</u>	<u>Page</u>
3.1	Current Materials Considerations . . . . .	3-10
3.2	Thermochemical Cycles . . . . .	3-19
3.3	Electrical and Thermal Requirements for Various Cycles Based on HTGR Heat Sources . . . . .	3-20
3.4	Design Parameters for the TMR . . . . .	3-26
3.5	A Parametric Study on Varying Decomposer Temperature . . .	3-53
3.6	Comparison of Conversion and Transport Options. . . . .	3-64

3. EXECUTIVE SUMMARY

3.1 Summary of Our Findings

We report on a scoping design study of a fusion reactor based on tandem mirror physics coupled to thermochemical processes for the production of hydrogen. The work is a result of a collaboration between the Lawrence Livermore National Laboratory, the University of Washington, and the Exxon Nuclear Company, Inc.

This study was accomplished between October 1, 1979, and September 30, 1980, under the auspices of the Office of Fusion Energy, U.S. Department of Energy.

In summary form, our findings were as follows:

- The production of hydrogen using thermochemical cycles has a demonstrated experimental base at the laboratory level. Production rates of 100 liters/hour are being achieved. Potential drivers for these processes, producing a vital energy source, are limited. There are only three:
  - (a) The fusion reactor
  - (b) The HTGR or VHTR
  - (c) Solar
- Of the three drivers, the fusion reactor and the HTGR would appear to have an edge over solar concentrators, due to the diurnal nature of solar and the need for thermochemical cycle production to be on a continuous 24-hour basis.
- The reasons for using a fusion reactor in preference to an HTGR for synfuel production were not obvious within the context of this study. Either could do the job. Both may

be appropriate. If fusion/electrical eventually supersedes or makes unnecessary HTGR/electrical, then it would seem that fusion/synfuel would follow.

- Relative to fusion reactor types selected for synfuels, the Tandem Mirror Reactor has an advantage over the Tokamak, due to the Tandem's energy output as thermal and dc electrical.
- If, in the first place, fusion makes sense for electrical energy production, then it is our finding that it is a reasonable extension that it be used for fuel production.

Taken collectively the design of a synfuel plant is extremely complicated. It is large--like an oil refinery--and has many difficult units to design. Where we were encouraged was in looking at the individual parts, rather than the whole, and concluding that the parts perceived to be the most difficult--the  $\text{SO}_3$  decomposer, the  $\text{H}_2\text{SO}_4$  boiler, and the fusion reactor blanket--all have good design possibilities. It is an exciting area and one just beginning to be explored. Even in the short time of a one-year scoping study at fairly modest funding, we have made good progress on component design.

- The Fusion Reactor/Synfuel Plant complex is substantially more difficult to analyze than a Fusion Reactor/Electrical Plant Complex. With fusion/synfuels virtually all parameters are interactive and closely coupled. With fusion/electrical one need only be concerned with the nuclear island, since the technology for the balance of plant exists.
- High temperature is the principal distinguishing parameter vis-a-vis hydrogen or electrical production. The thermochemical ( $\text{H}_2$ ) processes studied required the delivery

of process heat  $\sim 1100$  K to 1200 K, compared to fusion/ electric at  $\sim 750$  K.

- To relax the temperature demands in the reactor area and in the transport area (for reductions of several hundred degrees) it is possible to burn or oxidize a portion of the hydrogen product in-situ at the  $\text{SO}_3$  decomposer, the highest temperature process unit. This hydrogen recycle decreases efficiency, but this loss may be more than compensated for by resolution of critical, high temperature materials problems.
- A similar result to the hydrogen recycle may be accomplished by using excess dc electricity (a unique feature of the Tandem Mirror Reactor with its direct convertor) to Joule heat the  $\text{SO}_3$  decomposer to the required high temperature. This is an extremely interesting possibility for the TMR/Synfuel tie and could be used independently or in conjunction with some hydrogen recycle.
- Tandem Mirror Reactor confinement physics for synfuel/hydrogen production is substantially the same as that for electrical production. There is some gain in reactor Q (the reactor figure of merit defined as fusion power produced divided by injected power), and some economies of size to be realized with synfuels. This is because of the larger reactor required for the synfuel plant.
- The key engineering problem in the reactor (without resorting to the Joule heating or the hydrogen recycle) is the ability to design a high temperature ( $\sim 1200$  K) blanket module. We studied two types:
  - (a) a binary, Li-Na liquid metal Cauldron module
  - (b) a flowing lithium oxide microsphere blanket.

Sintering of particles, high temperatures in the zone dividers, and complicated heat transfer preclude the use of the flowing microsphere blanket at this temperature. The highly-modularized, low-stress Cauldron design has many positive attributes, but requires experimental verification of MHD effects and a clearer understanding of energy transfer within the pool.

- Integral tritium production, control, and removal at our elevated 1200 K temperature appears achievable in either blanket design, as compared with previous reports by others where tritium production had to be done in a separate, lower temperature region of the blanket.
- The percentage of process heat delivered at high temperature (1200 K) turned out to be excellent, ~90%, for either blanket design. This represents a very effective use of the reactor as a heat source.
- Transporting the process heat to the thermochemical plant using sodium as the heat transport fluid presents severe corrosion and safety problems, but is a good option considering stresses (pressures can be balanced) and temperature retention (film temperature drops are low). The technology would be an extension of LMFBR technology.
- Transporting the process heat using helium has the great advantage of safety and inertness. The price paid is higher pumping power, higher stresses (pressures cannot be balanced), and some additional loss of temperature (film temperature drops are high).
- The materials problems at high temperature and in corrosive atmospheres are difficult. However, we are encouraged by our findings summarized in the following Table 3.1.

TABLE 3.1 CURRENT MATERIALS CONSIDERATIONS

<u>Material</u>	<u>Application</u>	<u>Pros and Cons</u>
V Alloys	<ul style="list-style-type: none"> <li>● First Wall</li> <li>● Feltmetal Insulator</li> <li>● T Permeation Membrane</li> </ul>	<ul style="list-style-type: none"> <li>● Good resistance to radiation damage</li> <li>● Low Activation</li> <li>● Good corrosion resistance to liquid Li, Na, K</li> <li>● High T permeation rates</li> </ul>
Nb Alloys	<ul style="list-style-type: none"> <li>● T Permeation Membrane</li> </ul>	<ul style="list-style-type: none"> <li>● Good corrosion resistance</li> <li>● High T permeation rates</li> </ul>
β-Ti Alloys and Ti-V Alloys	<ul style="list-style-type: none"> <li>● First Wall</li> <li>● Feltmetal Insulator</li> <li>● Cauldron Wall</li> </ul>	<ul style="list-style-type: none"> <li>● Resistance to radiation damage is probably good</li> <li>● Low activation</li> <li>● Good corrosion resistance to liquid Li, Na, K</li> <li>● High T diffusion rates</li> </ul>
Mo Alloys (TZM)	<ul style="list-style-type: none"> <li>● Heat Pipes</li> <li>● Heat Exchangers</li> </ul>	<ul style="list-style-type: none"> <li>● Very high strength</li> <li>● Excellent heat conductivity</li> <li>● Excellent corrosion resistance to liquid Li, Na, K</li> <li>● Good small-scale fabricability</li> <li>● Problems in large-scale fabrications</li> </ul>
In-800	<ul style="list-style-type: none"> <li>● Transport piping for Liquid La, K</li> </ul>	<ul style="list-style-type: none"> <li>● Good creep strength to 1100 K</li> <li>● Good corrosion resistance to liquid Na, K</li> </ul>
In-800H	<ul style="list-style-type: none"> <li>● Heat Exchangers</li> </ul>	<ul style="list-style-type: none"> <li>● Aluminate-coated In-800H shows good corrosion resistance to SO<sub>2</sub></li> </ul>
Siliconized SiC	<ul style="list-style-type: none"> <li>● Heat Exchanger for Boiler</li> </ul>	<ul style="list-style-type: none"> <li>● Excellent compatibility with boiling H<sub>2</sub>SO<sub>4</sub> at 673 K</li> <li>● Compatibility with liquid Na or K</li> </ul>

## 3.2 The Technical Choice of the TMR

### 3.2.1 The Confinement Physics

A primary technical (topological) reason for choosing the tandem mirror was its highly favorable reactor configuration. As shown schematically in Fig. 3.1 from a physics perspective, the reactor consists of a long central cell in which the power-producing high-beta (0.4) D-T plasma is confined by straight magnetic field lines that are produced by simple, circular Nb-Ti superconducting coil modules. In our design study, these coils are about four meters apart and the central cell length is 213 meters.

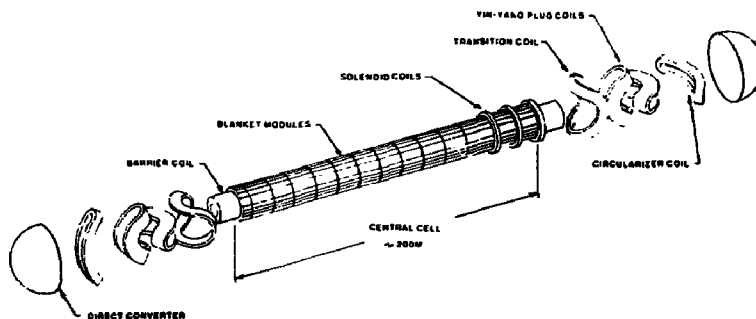


Fig. 3.1 Tandem mirror reactor with thermal barriers.

The power producing plasma of the central cell is electrostatically confined at its ends by the plasma in the yin-yang end "plugs", each of which is a minimum-B stabilized mirror.

Figure 3.2 illustrates the axial variation of both the magnetic field and electrostatic potential in a tandem mirror with thermal barriers, corresponding to the magnet arrangement of Fig. 3.1. The vacuum magnetic field  $B_{op}$  of the plug is larger than the magnetic field  $B_{oc}$  of the central-cell in order to provide magnetic-mirror confinement of the central-cell plasma. The plugs themselves are magnetic mirrors, as indicated by the dips in their magnetic field profiles. Plasma electrons, because of their higher thermal velocity, escape the central cell faster than the ions. This tendency charges the central cell positively by an amount  $\phi_e$ . This ambipolar potential then holds the electrons back. Similarly the plugs charge positively to a potential  $\phi_p = \phi_e + \phi_c$ . This is the basic idea of tandem-mirror. It makes use of the positive potential  $\phi_c$  of the plugs with respect to the central-cell to repel and prevent escape of central cell ions.

An improvement to the basic tandem mirror was the addition of what are called thermal barriers. The thermal barriers at each end between the central cell and the end plugs are formed by  $Nb_3Sn$  barrier coils which apply large magnetic mirrors at the ends of the central cell, but inside the end plugs. In our synfuel study, these barrier coils were 12 Tesla. The central-cell plasma spreads out along the radially expanding magnetic lines as it leaves the magnetic barrier field, and its density is thereby reduced in the barrier regions. Since the electrons are in thermal equilibrium, the electrostatic potential  $\phi$  and the electron number density  $n$  are connected by the relation  $n = n_0 \exp \left[ \frac{e(\phi - \phi_0)}{kT_e} \right]$ . Therefore, a dip  $\phi_b$  in electrostatic potential is induced in the barrier region, as shown in Fig. 3.2. This dip is a rise in potential energy for electrons and separates the plug and central-cell electron populations, thereby allowing them to have different temperatures. The ion density of the barrier is kept low by neutral

beams directed into the barrier region inside the central-cell loss cone. Trapped barrier ions are neutralized and escape, while the injected neutrals fuel the central-cell as charge-exchange fast ions. Electron-cyclotron heating is applied to the inside of each plug, thereby raising  $T_e$  and allowing the plug potential to rise as shown in Fig. 3.2. This provides the potential barrier for central-cell ions without excessive plug density and without requiring high values of central-cell  $T_e$ .

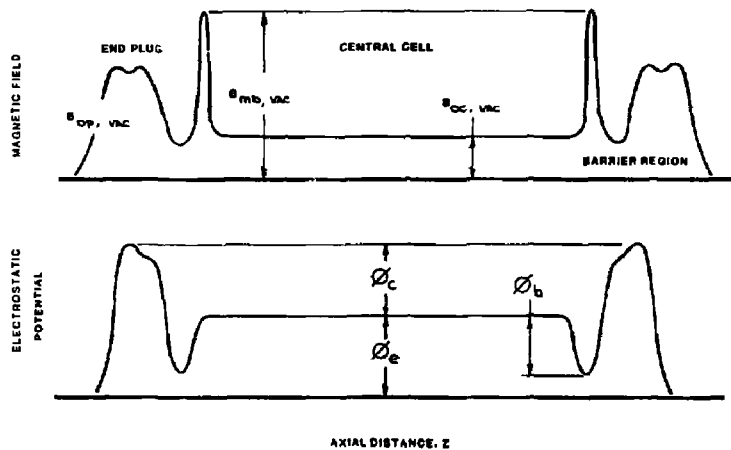


Fig. 3.2 Axial magnetic field and electrostatic profiles in the Tandem Mirror with thermal barriers

### 3.2.2 The Engineered Reactor Topology

As an engineered reactor, the topology created by confinement physics of the TMR not only allows the design of relatively simple blanket modules, that are the principal source of the process heat used for hydrogen production, but permits putting all the modules together into a workable package along the central cell length.

The sequence of figures that follow, Figs. 3.3 A, B, C, D, and E; illustrates how the blanket modules, tailored for the synfuel thermochemical cycle use, may be assembled into a serviceable, accessible reactor for producing energy.

### 3.3 The Tandem Mirror Reactors Energy Forms

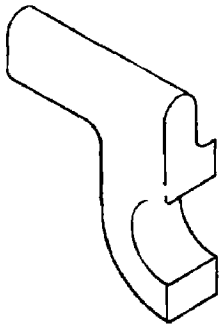
The Tandem (TMR) is a steady-state, driven fusion device. Energy from the reactor is produced in two primary forms, as evidenced by equation 3.1.



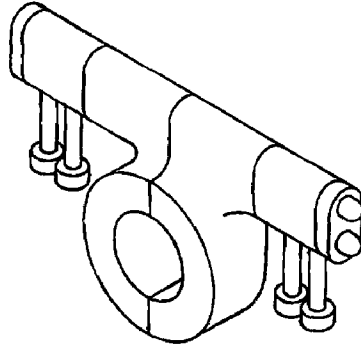
Deuterium + Tritium → Energetic Neutron  
+ charged particle

The first energy form, the kinetic energy of the neutron, is captured in the moderating blanket surrounding the reacting plasma, and thermal energy is produced. The neutrons, as they are moderated in the blanket, produce some additional energy by exothermic neutron-lithium reactions.

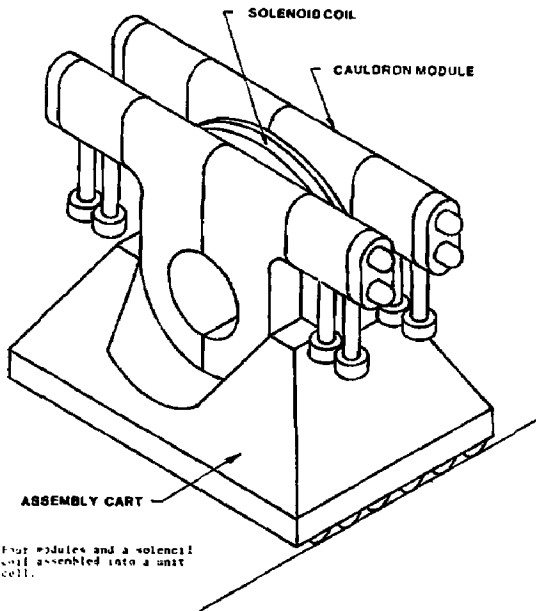
The second energy form produced by the reactor is that contained in the charged alpha particle. On forming, the alpha begins to lose some of its 3.5 MeV energy by heating the plasma



Basic geometry of a  
Cauldron blanket module.



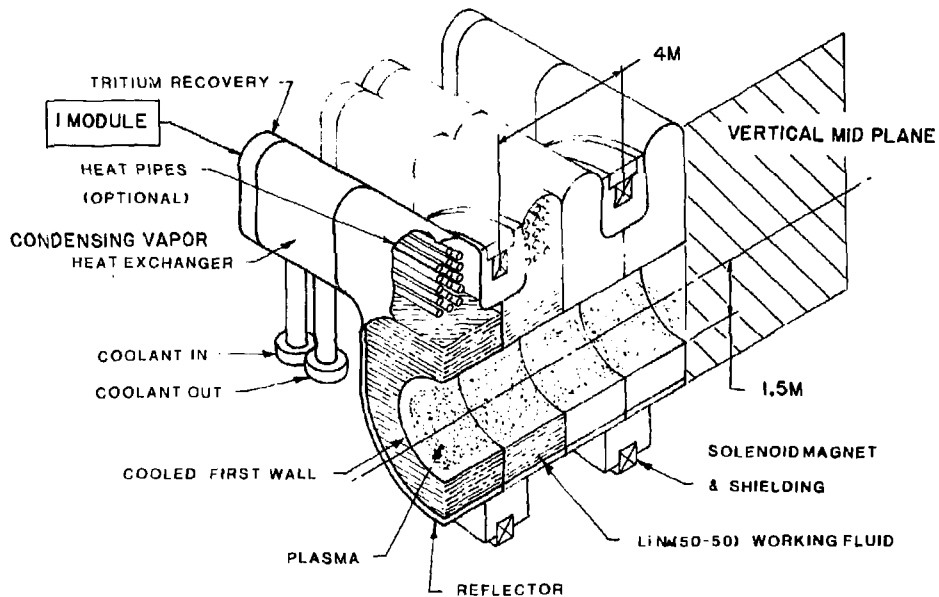
Four modules joined  
and ready for assembly  
with a central cell  
blanket.



Four modules and a solenoid  
coil assembled into a unit  
cell.

Fig. 3.3 A, B, and C Assembly of Blanket Modules

## CROSS SECTION THRU 2 UNIT CELLS



3-16

Cross section through two unit cells of the FBR. Each unit cell consists of four blanket modules and one solenoidal coil. The unit cells are joined in series to form the main central cell of the reactor. The axial distance between coils is approximately 1.5 meters.

Fig. 3.3 D Assembly of Blanket Modules

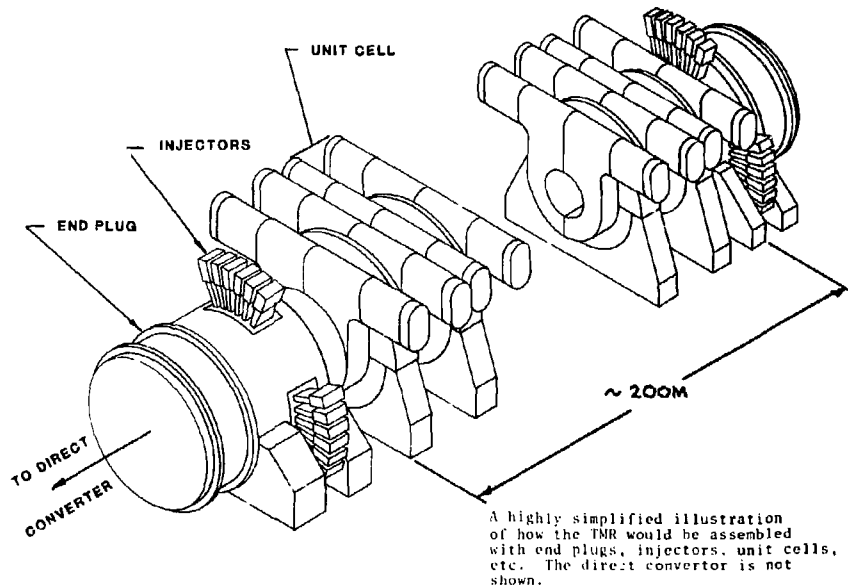


Fig. 2.3 E Assembly of Blanket Modules

through a series of collisions with electrons and ions. Finally, at some degraded energy, the alpha particle leaves the system (the central cell) through the ends as do the deuterium and tritium ions that did not react with one another. All the alpha particle energy may now be accounted for as the sum of its residual energy plus the enhanced energy of the exiting deuterium and tritium ions. This energy is recovered as dc electricity in a direct convertor located beyond the end cells, as suggested in Fig. 3.1. The direct convertor actually produces two forms of energy: the electrical dc component, which we use in this particular scoping design to drive the reactor, and a thermal component which, for our thermochemical cycle, supplements the blanket energy that is used for the process chemistry to produce our hydrogen product.

The availability of both of these energy forms, thermal energy and dc electricity, is unique to open-ended fusion machines, as compared with closed topology systems such as the tokamak. This availability can be of distinct advantage in synfuel production via thermochemical cycles and will be discussed subsequently.

#### 3.4 The Energy Needs of the Thermochemical Cycles

In this study we investigated and considered three thermochemical cycles, shown in Table 3.2, whose chemistry and closed loop operation had been verified in the laboratory.

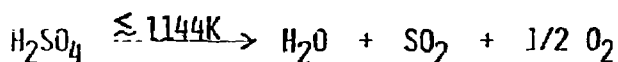
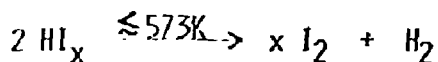
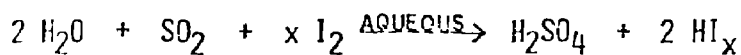
We have selected one of the three, the General Atomic sulfur iodine cycle, for our initial scoping design study.

The current electrical and thermal requirements for these three cycles are shown in Table 3.3. It is to be noted that all three of these cycles have substantial electrical demands, although

TABLE 3.2

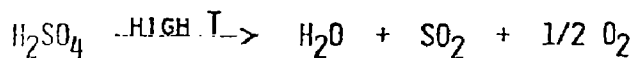
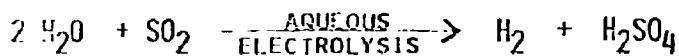
THERMOCHEMICAL CYCLES WHOSE CHEMISTRY AND CLOSED LOOP  
OPERATION HAVE BEEN VERIFIED IN THE LABORATORY

SULFUR-IODINE CYCLE



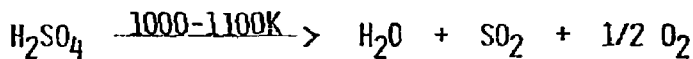
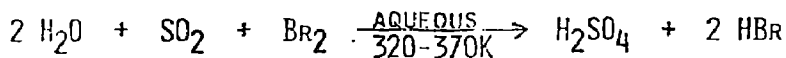
GENERAL  
ATOMIC

SULFUR CYCLE (PART ELECTROCHEMICAL)



WESTINGHOUSE

SULFUR-BROMINE CYCLE (PART ELECTROCHEMICAL)



EURATOM  
ISPRA

TABLE 3.3 ELECTRICAL AND THERMAL REQUIREMENTS FOR VARIOUS CYCLES  
BASED ON HTGR HEAT SOURCES

Thermo-chemical Cycle	Thermal Eff.	Process Heat		Thermal energy used to generate electricity or shaft work	
		High Temp.	Intermed. Temp.	Electrolytic Demand	Process Shaft Work
General Atomic	47%	24%	51%	0	25%
Sulfur Iodine		1250 K	843 K		
Westinghouse	47%	23%	20%	57%	0%
Sulfur Cycle		1280 K	1108 K		
ISPRA	46%	27%	52% below 773 K	21%	0%
Mark-13		1083 K			

the processes are generally described as thermochemical. The GA cycle, although it does not have an electrolysis step, nevertheless requires roughly 25% of its energy in electrical form. This electrical requirement will be seen to be an advantage for high Q tandem mirror reactors with their inherent dc electrical output, particularly with advanced fuel cycles.

### 3.5 The Tandem Mirror Reactor Energy Balance, Thermal and Electric

For the thermochemical cycles, as Table 3.3 indicates, there is a need for both electrical power production and the production of process heat from the fusion reactor. We have indicated that

two regions of the tandem mirror fusion reactor provide this process heat: (1) the blanket and (2) the thermal part of the direct convertor, while surplus electrical energy out of the direct convertor over and above that required to drive the reactor can be used to satisfy the electrical demands. This surplus begins to occur at a reactor Q of about 11 for the reactor parameters we have chosen.

### 3.6 The Influence of Q on the TMR's Uniqueness

To fully appreciate the TMR as a unique energy source compared to other sources (Fig. 3.4) for synfuel ( $H_2$ ) production, one must examine the fusion gain, Q, of the reactor as a parameter associated with the energy balance of Fig. 3.5. The Q is defined as fusion power produced divided by the injected power to produce it. We have stipulated for our scoping study that the dc electrical energy component  $B\eta_{dc}$  of the direct convertor will be used in the first place, to exactly satisfy the circulating power and the auxiliary needs of the reactor itself. This meant simply that the dc component of the direct convertor drives the reactor and the ancillary equipment. No other energy input is required. As can be surmised, there will be a specific value of Q at which this demand is exactly satisfied. For higher Q values, there will then be a surplus of dc electrical energy that will then be used by the thermochemical plant. For lesser values of Q, some thermal energy from the reactor blanket or from the thermal part of the direct convertor would have to be converted to electrical energy to help drive the reactor. Fig. 3.6 is a plot of how this electrical surplus or deficiency,  $P_{dc} - (P_{aux} + P_{circ})$ , varies as a function of Q. It may be seen from Fig. 3.6 that when the Q value is about 11 or higher, there begins to be a dc electrical component that can be used to drive such things as pumps, motors, etc. in the synfuel plant or possibly Joule heat the high temperature  $SO_3$  decomposer.

OVERALL EFFICIENCY POTENTIAL OF DIFFERENT ENERGY SOURCES

o Tandem D-T cycle

$$\eta_{net} = 0.8 \eta_{th} + 0.2 [\eta_{dc} + (1-\eta_{dc}) \eta_{th}]$$

$$\eta_{net} \approx 0.32 + 0.146 \approx 47\%$$

o Tandem D-D Cycle

$$\eta_{net} = 0.5 \eta_{th} + 0.5 [\eta_{dc} + (1-\eta_{dc}) \eta_{th}]$$

$$\eta_{net} \approx 0.20 + 0.365 \approx 57.5\%$$

o Tokamak D-T Cycle or D-D cycle, the HTGR or a Solar Concentrator

$$\eta_{net} = \eta_{th}$$

$$\eta_{net} = 0.40 \approx 40\%$$

Fig. 3.4 The tandem mirror reactor energy source compared with other energy sources

**POWER BALANCE-MIRROR REACTOR  
WITH DIRECT CONVERSION PROCESS  
HEAT PRODUCTION FOR SYNFUELS**

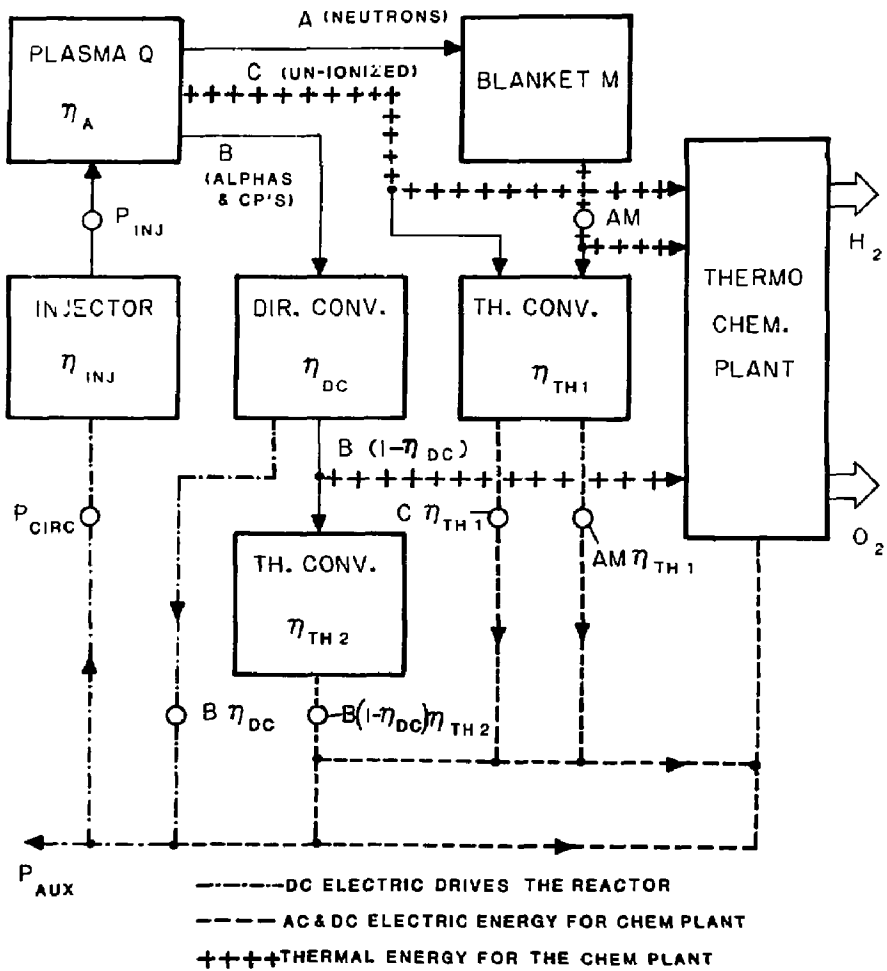


Fig. 3.5 Energy balance--Tandem Mirror Reactor

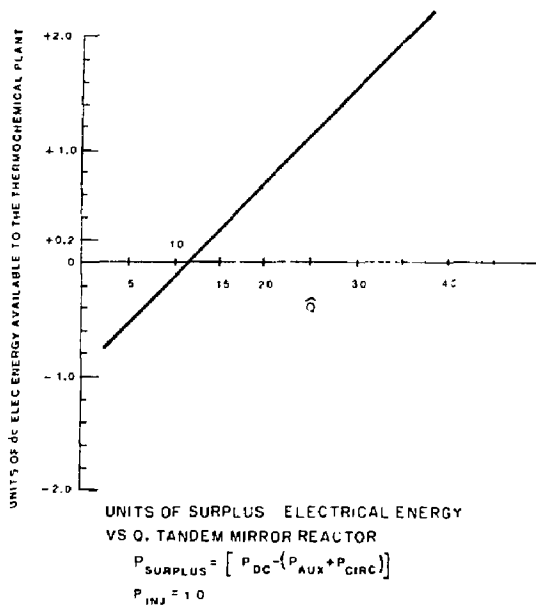


Fig. 3.6 Units of surplus electrical energy vs Q for the TMR

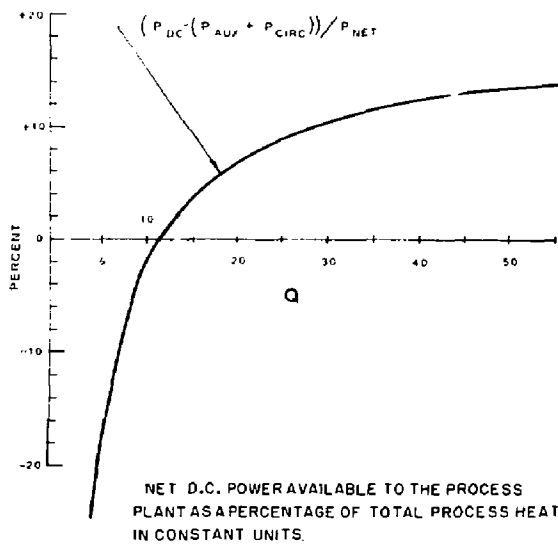


Fig. 3.7 Net dc power available to the Process Plant as a percentage of total process heat

Relative to the total energy that the reactor has created for synfuel purposes, the fraction that is dc tends to a limit R, where R is defined as surplus dc (expressed in units of equivalent thermal energy) divided by the total energy available to the process chemistry. This limit is indicated in Fig. 3.7, where we see that as Q gets larger and larger, the dc percentage of the reactor's output available for process chemistry tends to a limit of about 13% for the D-T cycle. More advanced cycles, such as D-D, D-He<sub>3</sub>, have higher limits on direct electrical energy production.

### 3.7 Conclusions on the Tandem as an Energy Source for Synfuels

From Figs. 3.6 and 3.7 some conclusions can be reached.

- 1) At a Q value  $\sim 11$ , the TMR dc electrical output is just large enough to feed back and drive the reactor, leaving the thermal fraction of the direct convertor and the blanket thermal energy available for process chemistry.
- 2) As Q values exceed 11, there is some surplus dc electrical power available for process chemistry.
- 3) As Q increases, the direct current electrical energy that is available for process chemistry tends to a limit of about 13% of the reactor useful output.
- 4) The availability of this direct current electrical energy from the TMR is an asset that other energy producing machines do not have. The HTGR, the Tokamak, the LWR, the FBR -- all of these machines must go through the thermal conversion step to produce this electricity at a penalty that is directly proportional to the thermal efficiency. The tandem begins to avoid the thermal step when values of Q exceed 11.

- 5) Advanced cycles have even a greater potential for direct electrical energy production.

### 3.8 TMR Design Parameters - Thermochemical Hydrogen vs Electrical Production

Table 3.4 provides a comparison between our scoping conceptual reactor design for fuel production and one for electrical production.

TABLE 3.4 DESIGN PARAMETERS FOR THE TANDEM MIRROR REACTOR (CF. SECTION 4.4.3) AS A DRIVER FOR THE HYDROGEN SYNDFUEL PLANT AND AS AN ELECTRICITY PRODUCER

	<u>Synfuel</u>	<u>Electricity</u>
Fusion Power (MWf)	3850	3500
Thermal Power (MWt)	3485	3360
First-Wall Loading (MWn/m <sup>2</sup> )	1.5	2.6
ECRH Power (MW)	248	260
Neutral-Beam Power		
Central-Cell (MW)	0	0
Barrier Cell (MW)	73	58
Plugs (M)	7.4	48
Central-Cell Length (m)	213	125
Central Cell First Wall Radius (m)	1.6	1.7
Central-Cell Beta	0.4	0.5
Reactor Q Value	11.6	9.6

### 3.9 Synfuel Influence on Reactor Design

It can be stated that the main and very significant influence synfuel production appears to have on reactor design has to do with blanket modules (and their associated heat exchangers, transport piping, etc.), those units surrounding the plasma that convert the neutron's kinetic energy to thermal energy, and in the case of the D-T cycle also produce the tritium part of the fuel by neutron-lithium reactions. Blanket moderating fluids (or solids) appropriate to hydrogen fuel production must run hot--1200 K is representative; whereas, blankets for electrical production could run hot, but need not--750 K is typical.

Materials problems arise as a consequence of the higher blanket temperature. The bulk of the other engineering elements of the reactor: neutral beam injectors, magnets, electron cyclotron resonance heating, shields, etc. remain the same as they would be for electrical production. The reactor physics for synfuels may be slightly easier due to the basic size difference of a fusion reactor driving a synfuel plant compared to a reactor for electrical production. A synfuel plant is likely to be larger, by perhaps a factor of 2, than an electrical plant. Thus the reactor Q, the figure of merit, can become higher because it is a function of length. Economics of scale are also implied by the larger size.

### 3.10 The Reactor Blanket Designs

Two basic high temperature blanket module concepts were considered in this study. One is the Li-Na Cauldron blanket. The other is the flowing microsphere design.

#### 3.10.1 The Operating Principle of the Cauldron Blanket Module

A cross-sectional view and an isometric view of the Cauldron module are shown in Fig. 3.8 A & B. Notice the module's resemblance to a pool boiler. It is, however, substantially more complicated than a pool boiler due to geometric effects, due to the exponential energy generation in the fluid contained within the module and, last, but not least, due to MHD effects on the convective mixing of the two liquid metals, lithium and sodium, we have chosen to use in the pool. The two liquids in this Cauldron module act as neutron moderator heat transfer fluid and tritium producer. Heat is removed by vaporizing the sodium. The sodium vapor, traveling at vapor velocities roughly 8-10 m/s at 1200 K, condenses on the heat exchanger tubes in the dome (the condensing vapor heat exchanger CVHX) and returns as liquid droplets to the pool, thus completing the cycle. In the dome,

**THE CAULDRON CONCEPT-HOUSING A HOT FLUID IN A COOL CONTAINER**

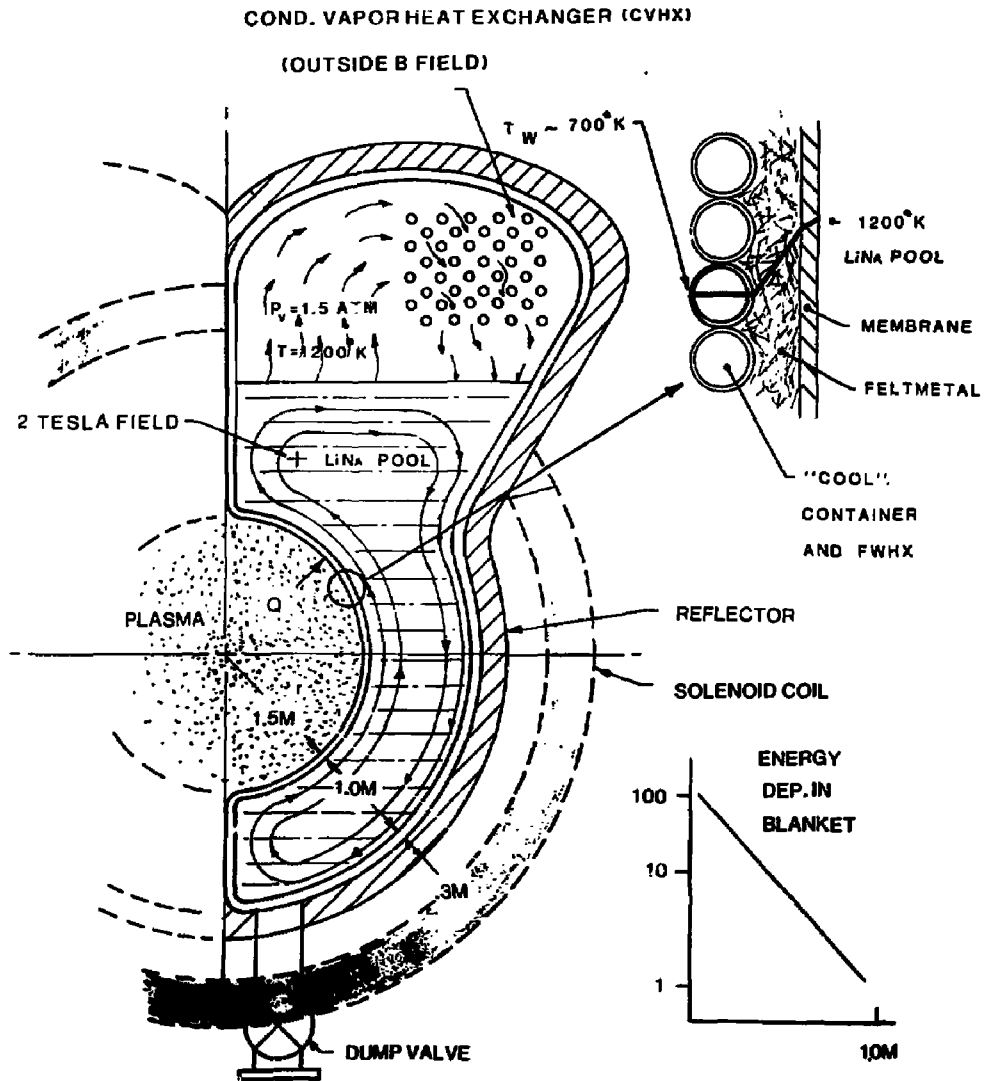
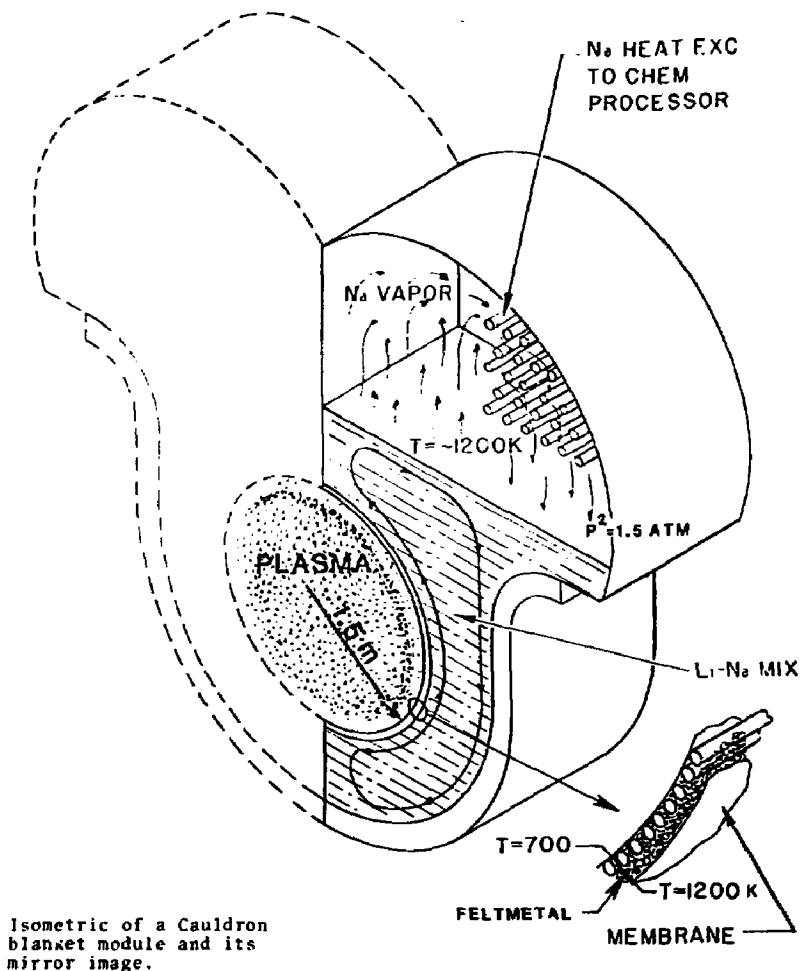


Fig. 3.8A Cross section and isometric view of the cauldron blanket module



Isometric of a Cauldron blanket module and its mirror image.

Fig. 3.8B Cross section and isometric view of the cauldron blanket module

the CVHX transfers the thermal energy out of the module to various chemical processors located some distance from the reactor.

Lithium and sodium are miscible, and tritium production with a 50-50 mix is greater than 1. LiK, LiRb or LiCs are other mixes or compounds that may be of future interest.

Success of this Cauldron concept depended in part upon our ability to contain the very hot fluid (1200 K) in a cool container. This was accomplished by establishing a steep temperature gradient across a thickness of material intervening between the hot fluid and the structural container itself. The material chosen was a commercial product called FELTMETAL, which can be fabricated to have an effective thermal conductivity  $k_e$  tailored to the needs of the problem. For our particular case the  $k_e$  was 0.175 w/mk. An important feature of the FELTMETAL is its substantial compressive strength and its low shear strength. Our Cauldron application loads the material in compression, due to the hydrostatic head of fluid and due to the sodium vapor pressure. The 500 K temperature gradient across the material, with the differential expansion it creates, is accommodated by allowing the FELTMETAL fibers to slide on one another. To establish the temperature gradient, in addition to controlling the FELTMETAL conductivity, we control the coolant flow in the first wall heat exchanger (FWHX) which is integral with the first wall structure, as may be seen from Fig. 3.8 A and B.

### 3.10.2 Materials Selections for the Cauldron

We have made initial selections of materials for the most critical elements in the Cauldron design, i.e., for the following:

- Cooled first wall portion of the structural envelope
- FELTMETAL insulator

- Cauldron wall (membrane)
- Condensing vapor heat exchanger
- Tritium permeation membranes

In selecting the materials, we have given major emphasis to neutron activation and radiation damage effects in materials close to the plasma and have further considered other factors such as corrosion, long-term creep strength, fabrication technology, and costs.

From the standpoint of low neutron activation combined with good radiation damage resistance, V and Ti alloys present the best materials prospects for the region near the plasma. Our current best choices for the first wall are V-10% Ti and V-20% Ti, since both of these alloys have been shown to suppress helium gas bubble formation. Further, triton impact should not cause problems of localized tritium buildup and blistering, since tritium is known to permeate very rapidly through V and its alloys. The technology of producing V alloy sheet and tubing and fabrication by electron beam welding is well established and presents no problems as long as interstitial O, N, and H are kept at low levels. The current cost of V is high (\$200/lb.), but V resources are extensive and cost reductions can be expected for quantity use. Even at \$200/lb., the cost is not excessive for the TMR first wall (~\$10M). Corrosion should not be a problem if liquid Na or helium is used as a coolant. If organic liquids (polyphenyls) are used, the coolant would need to be continuously purified to avoid carbon deposition in the tube passages due to radiation damage.

We are considering beta-Ti alloys as a backup material for the first wall. Although radiation damage information is sparse on these alloys, it is encouraging that hydrogen diffusivity has been shown to be substantially higher than in the alpha-Ti

alloys. For the cooled structural wall outside of the first wall region, a broad range of conventional low-cost alloys (e.g., Fe-Ni based alloys) are available, but have not been specified in this initial scoping.

For the FELTMETAL insulator, the beta-Ti alloys, Ti-13V-11 Cr-3Al, Ti-2.5 Al-16V, and Ti-7 Al-4 Mo are our current selections, based on existing commercial alloys. Improved Ti alloys or use of a Nb alloy layer next to the Cauldron wall may be necessary to avoid creep at the highest temperatures. It is envisioned that a helium sweep gas would be used to remove tritium from the porous FELTMETAL channel. This does not present a corrosion problem.

For the material of the Cauldron wall which is in contact with the liquid Li-Na pool and the resultant vapors, neutron activation remains of major importance; radiation damage effects are somewhat reduced (no triton impact) in the region near the plasma. Corrosion resistance becomes of critical concern throughout the Cauldron wall, and long-term creep (in spite of the low loading stresses) needs to be considered. We have selected the same commercial beta-Ti alloys for the Cauldron wall as for the FELTMETAL insulator. The corrosion resistance of pure Ti and of all of the alloying constituents except Al are known to be excellent in liquid Li, and the corrosion of Al is believed to be negligible because of its low diffusion rate through Ti. Also liquid L. is generally more corrosive than Na, so that we fully expect the beta-Ti alloys to have good corrosion resistance. We cannot give a definitive statement on the long-term creep strengths of beta-Ti alloys, due to lack of any direct data under the low-stress, high-temperature conditions encountered here. We are optimistic, however, in view of the fact that short-term tensile yield strengths (0.2% deformation) are quite high (33,000 psi) for Ti alloys such as MST 881

and Ti-8 Al-8 Zr-1 (Nb & Ta) at 1200 K. Fabrication and welding of both alpha- and beta-Ti alloys into large complex structures using electron beam welding techniques is a well-established technology in the aerospace industries.

The condensing vapor heat exchanger is sufficiently removed from the plasma region that neutron activation and radiation damage are no longer significant. The important materials considerations here are long-term creep resistance, high thermal conductivity, corrosion resistance to the Cauldron vapors and circulating heat exchange fluids, and ease of fabrication. The molybdenum alloy, TZM, is selected because of its outstanding behavior for the first three criteria above. Small-scale (up to 3 cm in dia.) welding of TZM for heat pipes and laboratory test capsules is well established and should be directly translatable to heat exchanger fabrication, although a larger scale technology has not yet been established. Certain developmental grades of Nb and Ta alloys would also be suitable for the heat exchanger, if the alloys were to go into commercial production. In-800 and In-800H also become acceptable if use temperatures are held to below 1100 K.

Tritium permeation membranes can be applied in several places depending upon the design specifics of the Cauldron and the heat transport loop, i.e., tritium needs to be removed directly from the Cauldron dome, from a processing slip-stream off the Cauldron dome, from the FELTMETAL channel, and from a liquid Na, liquid K, or gaseous helium heat transport loop. The vanadium, Nb, and beta-Ti alloys are selected as the preferred membrane materials because of a combination of high hydrogen permeability and good corrosion resistance to a Li-Na environment. Nb alloys are preferred at the highest temperatures where high strengths and low creep rates are required.

### 3.10.3 Conclusions and Observations on the Cauldron

1. The relatively simple configuration of the blanket module with its integral heat exchanger provides full plasma coverage when assembled into unit cells composed of one solenoidal coil and four blanket modules. The unit cells provide an attractive means for assembly/disassembly.
2. Neutronically, the Li-Na "boiler" portion of the module provides integral tritium generation and tritium recovery at the desired process temperature of 1200 K, rather than having to resort to a discrete but lower temperature zone in which the tritium is produced. This is an impressive feature of this design and makes it possible to achieve values for the energy fraction recovered at high temperature which are considerably greater than those typically reported previously.

The neutronics studies to date have assumed a Li-Na bath that is homogeneous and uniform. The heat transfer processes that occur, boiling in the bath and subsequent condensing on the integral heat exchanger will influence neutronics by bubble voids, temperature variations, etc., so that more elaborate, two-dimensional calculations will have to be performed.

3. The "cool container" concept of the Cauldron module appears to work quite well using the commercial FELTMETAL to establish the desired temperature gradient. The benefits are at least threefold:
  - The container need not be made from super alloys; we recommend that it be made from materials with a low residual activity, such as vanadium and titanium, as an environmental safety feature.

- The porous FELTMETAL allows gas sweep circuits that become part of the tritium removal and control.
- The division of total blanket energy between the cool structural container (FWHX) and the hot CVHX in the dome was found to be ~8%, 92%. Thus the energy partitioning is excellent.

The difficulty with the "cool container" concept is in selecting adequate materials for the membrane which separates the bath from the FELTMETAL and the structural envelope. Although the stresses are low in this membrane, it is subjected to the 1200 K bath temperature. The problems of long term creep on materials such as beta-titanium at this temperature must be assessed. This concern about membrane material and long term creep strength also applies to some fraction of the FELTMETAL immediately next to the membrane.

4. Fabrication and welding of large structural units such as the Cauldron model using electron beam welding has been established as a technology by the aerospace industries.
5. In the "cool container," which doubles as a first wall heat exchanger (FWHX) there is as yet no clear cut choice of a coolant. With sodium there is an MHD pressure drop induced of ~10 atm due to B field effects. Some degradation of blanket neutronics also occurs because of the sodium volume in the FWHX tubes. Fortunately, coolant tube diameters of 2 centimeters, required for other reasons, keep this sodium volume low. For helium as the coolant, the neutronics is better and helium is attractive as relatively inert gas. However, working pressures must be high, of the order of 50 atms; and stresses (diametral), created by large film temperature drops characteristic of gas flow, must be

watched carefully. The organic coolants (the terphenyls), not subjected to MHD effects and capable of operating at low pressure, have stability problems in a radiation field. The cure against instability may be more difficult than simply resorting to helium or sodium. The coolant choice for this FWHX needs further study and will certainly be influenced by coolants we use elsewhere, particularly in the condensing vapor heat exchanger, where the bulk of the flow occurs.

6. The condensing vapor heat exchanger (CVHX), located in the dome of the Cauldron module, is a fairly straightforward design problem. If sodium is the coolant, then pressures can be substantially balanced between condensate and coolant, and stresses will be low. The 1200 K process temperature level is also highly conserved for delivery to the chemical process equipment because of low film temperature drops both in the flowing coolant and in the condensate film. However, delivering large volumes of high temperature sodium (or potassium) to the process chemistry plant poses a difficult safety problem. Distances are likely to be long, ~100 m, and volumetric flow rates are high. Furthermore, bringing together in close proximity (separated only by a barrier wall) the sodium and the chemical process fluids and vapors, such as  $\text{SO}_3$ , may preclude the use of sodium. It is difficult to find a single metal container that can exist in both a sodium and a  $\text{SO}_3$  environment. If helium is used as the coolant in the CVHX, then there are pressure penalties and pumping power penalties one must accept.
7. The operational safety of the Cauldron module as a unit has been given serious attention since the handling of high temperature liquid metals is very difficult, even when there is no external flow. In the Cauldron module the binary

liquid metal, Li-Na, is well isolated within the module itself. One isolation barrier is the condensing vapor heat exchanger located in the dome. This heat exchanger can provide further isolation by the use of heat pipes between the condensate and the coolant flow. The "cool container" enveloping the boiling Li-Na fluid provides isolation via the membrane plus the tube wall itself. All the modules in the reactor are contained within a vacuum envelope. The exterior structure in which the total reactor is housed is imagined to be a steel-lined, two-meter thick, reinforced, concrete building, also under vacuum. Other safety features include quick-acting, gravity-activated dump valves for liquid metal removal from a module. Temperature and pressure sensors are provided in the dome and elsewhere to continuously monitor performance. The vapor dome itself provides a good buffer against inadvertent overpressuring.

8. Neutron/lithium produced helium can be removed from the Cauldron using a vapor dome processor.
9. Tritium produced in the blanket can be removed using catalytic oxidation and mole-sieve absorber processes operating on the blanket vapor dome, holding the total combined blanket tritium inventory to 1 kg. A slip-stream processor can hold the tritium loss through the CVHX into the thermochemical plant to 5 ci/d.
10. How well the Cauldron idea will work as a boiling heat transfer device is key to the success of this particular part of the fusion/synfuel study. There are insufficient data, both analytical and experimental, in this area of bulk fluid heating and boiling by internal heat generation from the neutrons. This is complicated further by the MHD effects of the B-field on the volume of the fluid and the MHD effects on the movement of the vapor bubbles within

it. Experimental verification of the Cauldron module performance is clearly essential before one could actually design an advanced pool-boiling fusion reactor blanket with high confidence. We have begun the design of a scale model which we plan to test in FY 81.

#### 3.10.4 Flowing Microsphere Blanket and Module Heat Exchanger

The flowing  $\text{Li}_2\text{O}$  microsphere blanket concept is an alternative to the Li-Na boiling Cauldron concept. The basic idea is to generate heat and breed tritium in the microspheres as they flow through the blanket. The hot microspheres then transfer their heat to a process working fluid in the module heat exchanger.

*The numerous advantages of such an approach to blanket design have been well documented in many earlier studies: simplicity, low operating pressures, high tritium breeding ratios, no MHD pressure drops, and shifting the bulk of the heat transfer to a region external to the blanket.*

In the simple baffled design the microspheres flow by gravity through radial zones where the flow velocity is controlled to produce a uniform average outlet temperature. A schematic description of a ten-zone design of this type is shown in Fig. 3.9 and additional modular detail, including a  $\text{Li}_2\text{O}/\text{Na}$  heat exchanger, is given in Fig. 3.10.

The radial gradient of the power density is approximately exponential. The variation in flow velocities required to achieve uniform average outlet temperatures in the ten zones range from 2.0 to 0.1 cm/sec. Such velocities should be achievable in a gravity-driven design by orificing at the exits. The radial dependence of the power density and the outlet temperatures are plotted in Fig. 3.11.

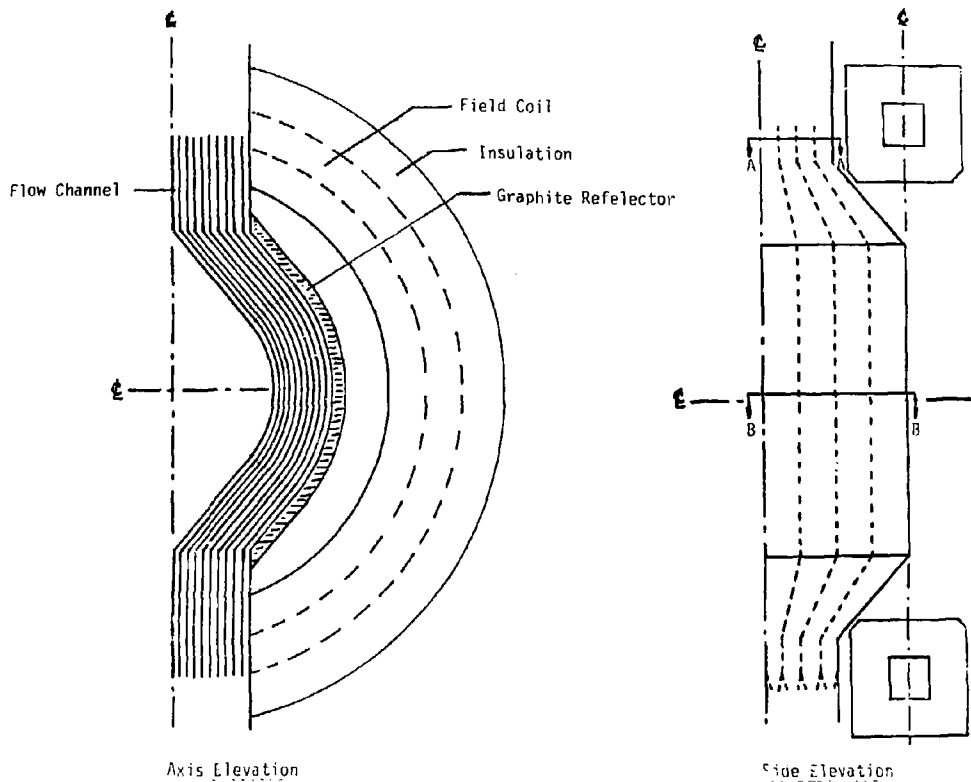


Fig. 3.9 Schematic Description of a Ten-Zone Flow Microsphere Baffled Blanket

50-5

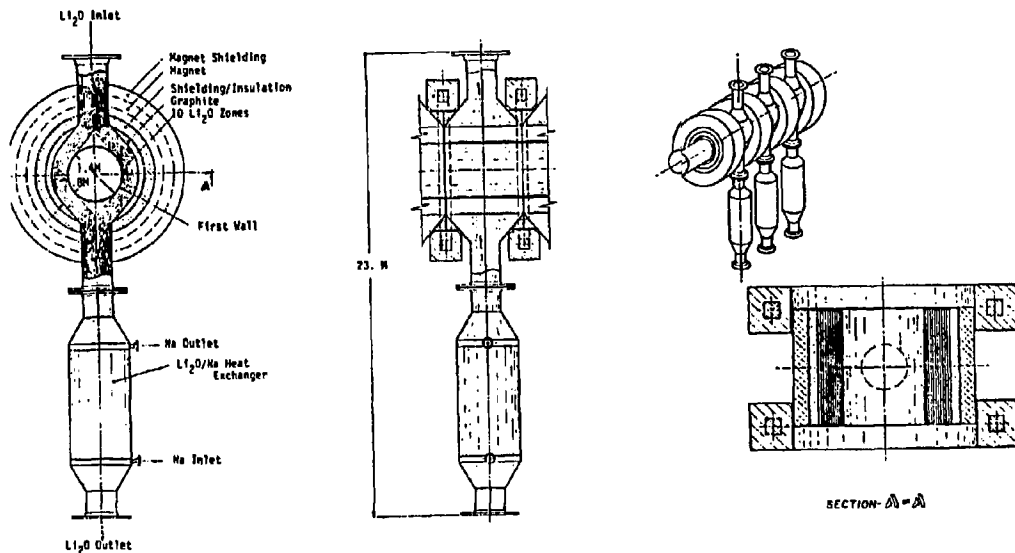


Fig. 3.10 Flowing  $\text{Li}_2\text{O}$  Blanket Concept Schematic for Thermal-Chemical Hydrogen Production

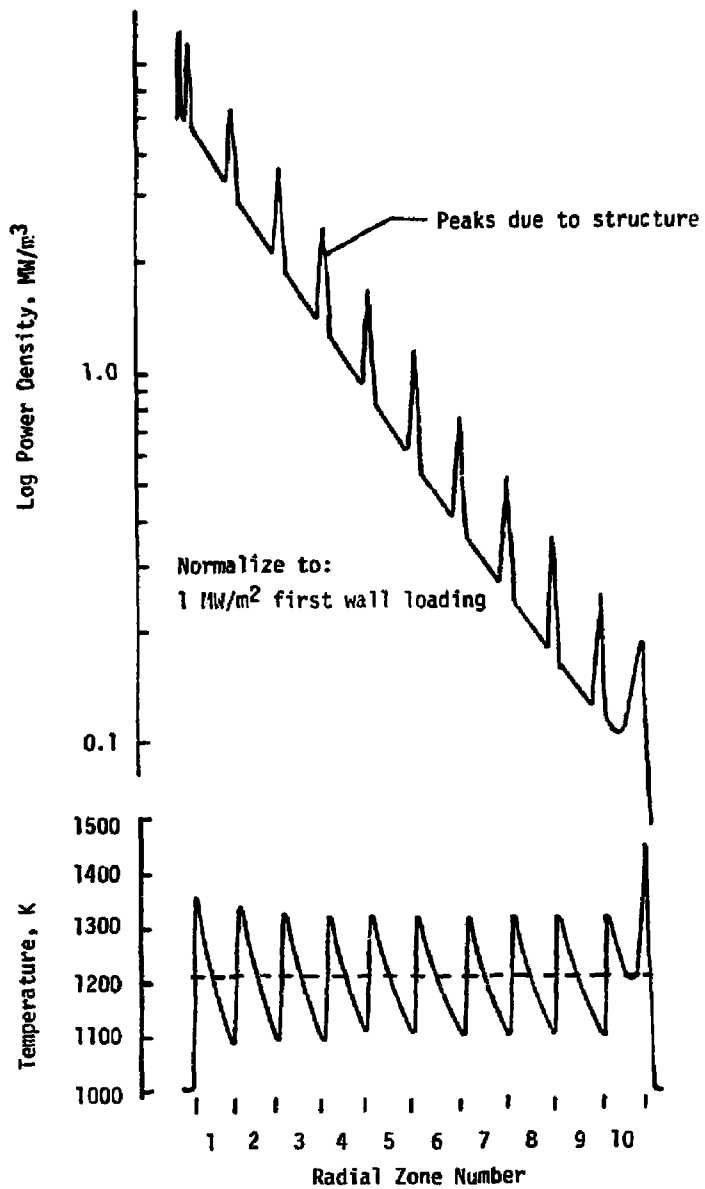


Fig. 3.11 Exit Temperature Distribution from Ten-Zone Blanket

If the baffle structure of this design is not cooled separately, the internal heat generation will produce local temperature peaking. The temperature distributions in the first set of baffles outside the first wall are shown in Fig. 3.12. The magnitude of the peaking in the remaining baffles is reduced because the power density in the structure decreases with radius.

The peak temperatures shown in Fig. 3.12 are too high for the use of conventional structural materials. Graphite is a possible candidate, but it is not clear that a credible design can be achieved. For this reason, a second  $\text{Li}_2\text{O}$  microsphere blanket configuration, the "cooled-tube," design, was also studied in some detail. In this design, the  $\text{Li}_2\text{O}$  flows through separately orificed insulated tubes. The heat generated in the structural material is removed by a separate He-cooling system. The results of the analyses of the cooled-tube design were not encouraging. The amount of structure required was large, about 40%. As a consequence, tritium breeding ratios were marginal, and the fraction of the heat recovered at high temperatures was substantially reduced, as compared with the simple baffled design. The cooled-tube design would also be much more expensive to build and more susceptible to radiation damage.

Detailed analyses of potential materials problems revealed several serious issues associated with operation at  $\text{Li}_2\text{O}$  temperatures at 1200 K in either of the blanket configurations. Sintering of the microspheres is probable at this temperature and almost certain to occur in hot spot regions. Vapor transport of  $\text{Li}_2\text{O}$  and  $\text{Li-OH}$  (or  $\text{Li-OT}$ ) is also an issue where such vapors could condense on cooler surfaces. Vapor transport could start at 1200 K and be quite active at 1400 K.

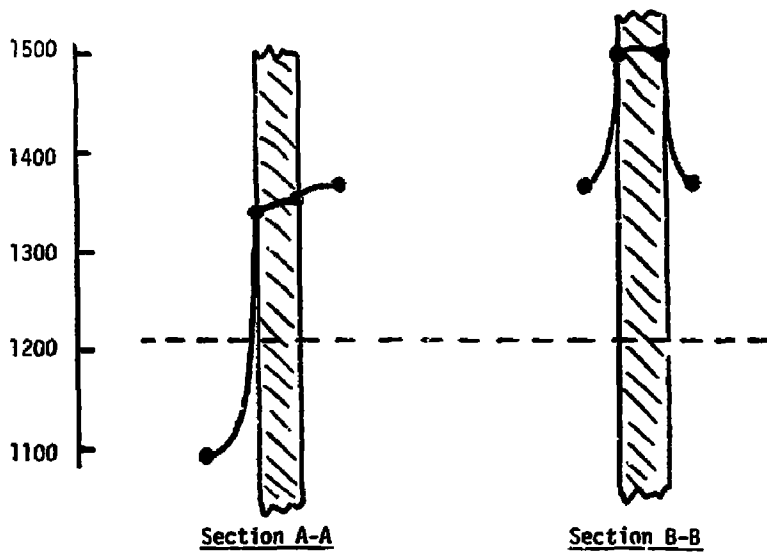
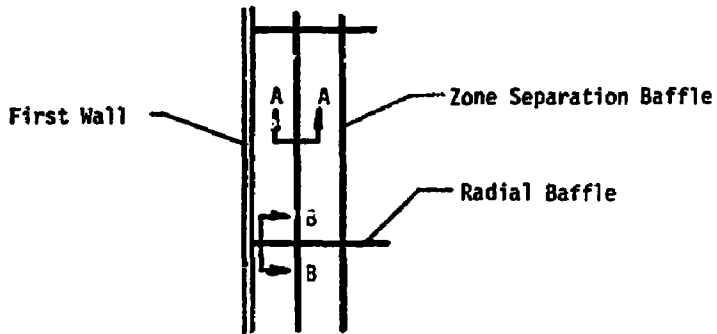


Fig. 3.12 Illustration of Temperature Distributions Through Uncooled Baffle Sections

The heat exchange of the  $\text{Li}_2\text{O}$  microspheres to the working fluid of the synfuel process is accomplished in a shell and tube heat exchanger. In one version, sodium is on the tube side and is heated from 615 K to 1160 K.  $\text{Li}_2\text{O}$  flows by gravity on the shell side and is cooled from 1210 K to 665 K. An alternative to the  $\text{Li}_2\text{O}$  heat exchanger would be one using helium.

The following conclusions can be drawn regarding the studies of the  $\text{Li}_2\text{O}$  flowing microsphere blanket designs:

1. A simple baffled design is very attractive in terms of structural simplicity, relatively uniform outlet temperature, high tritium breeding ratios, low operating pressures, and absence of MHD effects.
2. The baffled design involves temperature peaking in the baffle structure which may or may not be acceptable, depending on the  $\text{Li}_2\text{O}$  operating temperature.
3. The cooled-tube design is not an acceptable alternative for alleviating the temperature peaking problem because the large amount of structure required significantly reduces the fraction of the heat which can be recovered at high temperatures and makes tritium breeding marginal.
4. Operation with  $\text{Li}_2\text{O}$  microsphere temperatures at 1200 K does not appear to be feasible due to potentially severe problems of sintering and material transport. Operation at temperatures below 900 K is a feasible option.

### 3.11 Heat Transport System, Reactor to Thermochemical Process

We have considered both helium and sodium as candidates for the heat transfer medium delivering process heat from the reactor

to the thermochemical process. Either choice has pros and cons. The key features which should be highlighted in this executive summary are the problems of supplying this high grade heat over a substantial distance from the fusion reactor to the thermochemical plant and the associated operational costs and safety issues that result.

Sodium is thermal-hydraulically superior to helium when the sodium is outside of the influence of MHD effects caused by magnetic fields. Piping and pumping costs can be low. The use of hot liquid sodium piped throughout a thermochemical plant as one might pipe steam for process heat seemed to us to be marginally acceptable from a safety standpoint, since the working fluid for the thermochemical cycle is sulfuric acid. To alleviate this problem, we located the most heat demanding unit, the  $\text{SO}_3$  decomposer chemical reactor, and some steam generators adjacent to the fusion reactor, but in a separately isolated building. This is a partial solution. We were still left with safety issues, the most important of which involves a tube failure within the  $\text{SO}_3$  decomposer that could intermix the  $\text{O}_x$  and  $\text{H}_2\text{O}$  contained in the  $\text{SO}_3$  process stream with the liquid sodium. This could result in a fire or explosion. Similar safety problems with sodium-driven LMFBR designs have been studied. Application of LMFBR technology, such as the use of duplex tubes with annular gaps filled with helium, serves to isolate the two fluids and also provides a means of monitoring for leaks. This further minimizes the problem.

Helium was our alternate coolant to avoid the sodium problems. In exchange for offering safety from fires and explosions, helium presented problems of large pumping power demands and the need to operate at high pressure (i.e., 30 to 60 atm). Locating the  $\text{SO}_3$  decomposer and some steam generators in close proximity to the fusion reactor was helpful in keeping the pumping power under 5% of the reactor thermal output. The

high operating pressure of 30-50 atm appears to be manageable in the  $\text{SO}_3$  decomposer using the alloy Incoloy-800H, the same tube material used with sodium. Thicker tube walls and the need for twice as many tubes would add to the cost.

### 3.12 Thermochemical Plant Process

#### 3.12.1 Basic Principles of Thermochemical Cycles

A thermochemical cycle for hydrogen production is a process in which water is used as a feedstock along with a non-fossil high temperature heat source to produce  $\text{H}_2$  and  $\text{O}_2$  as product gases. The water splitting process is accomplished through a closed loop sequence of chemical reaction steps in which the chemical reagents are continuously recycled and reused in the process with essentially no loss of material. Practical thermochemical cycles, as currently envisioned, require input temperatures of  $\sim 1200$  K for the highest temperature chemical step and operate at a thermal efficiency of  $\sim 45\%$ . The thermal efficiency is defined as the higher heating value of the  $\text{H}_2$  produced, 286 kJ/g mol  $\text{H}_2$  (combustion enthalpy of the  $\text{H}_2$  to give liquid water at 298.15 K) divided by thermal heat delivered by the heat source.

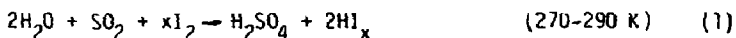
Of the approximately 30 cycles under study world-wide, only three cycles have thus far been developed to the stage where closed loop table-top models have been built and tested in the laboratory, and these are the cycles that we are considering for magnetic fusion applications. They were previously illustrated in terms of their principal chemical steps and reaction temperatures in Table 3.2. The main effort on the development of the Sulfur Iodine Cycle is underway at the General Atomic Company; for the Sulfur Cycle, at the Westinghouse Electric Corporation; and for the Sulfur-Bromine Cycle, at the

Commission of European Communities Joint Research Centre Ispra Establishment.

We compared these leading candidate thermochemical cycles and concluded that the G.A. cycle offered the logical first opportunity for our effort at coupling the cycle to our TMR since it did not utilize an electrolytic step, had relatively low electrical demands, and involved simple chemical engineering unit operation.

### 3.12.2 Chemical Description of the General Atomic Cycle

The Sulfur-Iodine Cycle being developed by the General Atomic Company is a pure thermochemical cycle operating in an all liquid-gaseous environment and is described by the following major reaction steps:



Major parts of the process are associated with separation and purification of the reaction products. A critical aspect for the successful operation of the process is in the separation of the aqueous reaction products in reaction (1). Workers at the General Atomic Company have solved this problem by using an excess of  $\text{I}_2$ , which leads to separation of the products into a lower density phase, containing  $\text{H}_2\text{SO}$  and  $\text{H}_2\text{O}$ , and a higher density phase containing  $\text{HI}$ ,  $\text{I}_2$  and  $\text{H}_2\text{O}$ .

Reaction (2) shows the catalytic decomposition of  $\text{HI}$ , which is in the purified liquid form (50 atm). Laboratory decompositions are around 30% per pass; therefore, a recycle step is

necessary. The unreacted HI is condensed out of the  $H_2$  and  $I_2$  products. Pure  $H_2$  is obtained by scrubbing out  $I_2$  with  $H_2O$ . The equilibrium for reaction (3) lies to the right at temperatures above 1000 K, but catalysts are needed to attain sufficiently rapid decomposition rates. Catalysts are available for this process, but careful consideration needs to be given to their costs versus effectiveness. Reaction 3, the  $H_2SO_4$  decomposition step, accomplished in a  $SO_3$  decomposition reactor, is a challenging unit to design owing to the high temperature and corrosive products involved. It should be noted that each of the three cycles shown in Table 3.2 requires this step. We have spent substantial time in this scoping study on a conceptual design of a fluidized bed  $SO_3$  decomposer, which we believe may be superior to previous designs.

### 3.12.3 The Fluidized Bed $SO_3$ Decomposer

The  $SO_3$  decomposer is a critical process unit in nearly all of the viable thermochemical plants that produce  $H_2$ . These plants can be driven by high-temperature gas-cooled reactors, solar collectors or fusion reactors with sodium, potassium, or helium. These heat transfer fluids supply the large heat demand of the  $SO_3$  decomposer by means of heat exchangers that are an integral part of the decomposer. Catalysts are required in this decomposer to keep the required temperature down to levels of  $\sim 1050$  to 1150 K.

The background chemistry on the  $SO_3$  decomposition reaction includes work at Westinghouse, at the Nuclear Research Centre in Julich, Germany, General Atomic in San Diego, and the Joint Research Centre at Ispra, Italy. The theoretical effect of temperature and pressure on the  $SO_3/SO_2$  equilibrium in the presence of water vapor is available. At around 5 atm reactor exit total pressure and 1050 K, the fraction  $SO_3$  converted to  $SO_2$  is around 55%. We have picked 5 atm and 1050 K for the

SO<sub>3</sub> decomposer chemistry to reduce materials' problems in the decomposer and in the TMR blanket as much as possible. This 55% compares to G.A.'s 74% conversion at 1144 K.

A sensitivity study was done showing the tradeoff between equipment size and this level of SO<sub>3</sub> decomposition selected as a design basis. In reducing the conversion from G.A.'s 74% to our 55%, the volumetric vapor load only increases 7.4%, which has a very small impact on the size of the expensive multi-effect evaporator train.

Perhaps the most detailed studies of SO<sub>3</sub> reaction kinetics with varying residence time were done on the Fe<sub>2</sub>O<sub>3</sub> catalyzed system by the Commission of the European Communities, JRC-Ispra Establishment, Italy. Their results are reproduced in Fig. 3.13. They show percent conversion versus residence time defined as the catalyst volume divided by the volumetric flow at 273 K and 1 atm.

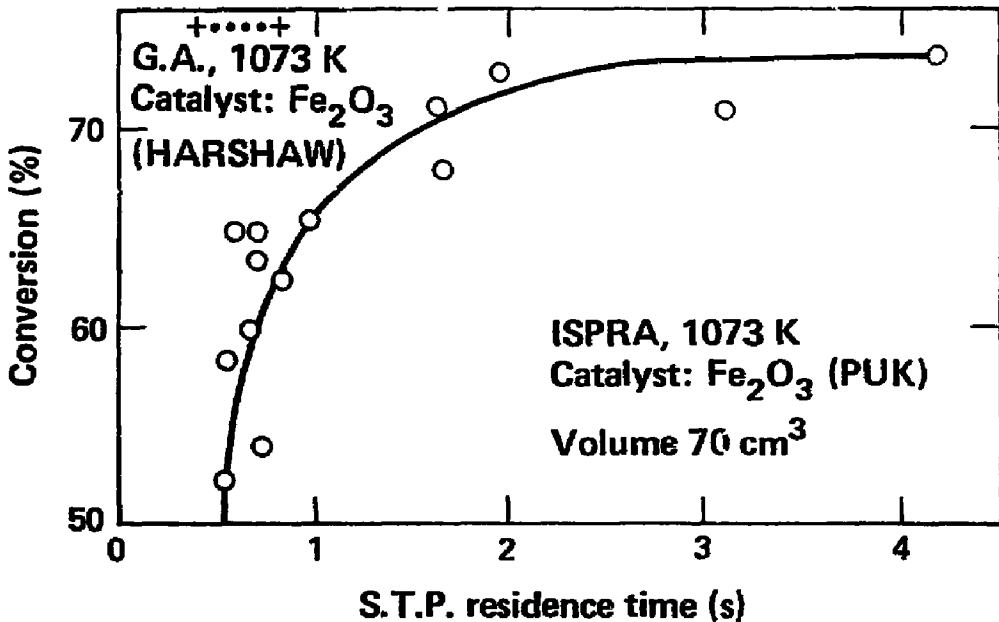


Fig. 3.13 Hydrogen production by decomposition of 95% H<sub>2</sub>SO<sub>4</sub>

For economic reasons we selected a low residence time, but consistent with high conversion. Ispra selected around 1 s at 64% conversion. Although residence times down to around 0.7 s appear feasible from Fig. 3.13, the steepness of the Ispra curve causes the conversion to be uncertain.

In G.A.'s studies, the residence time was varied from 0.2 s on up, and catalysts such as  $\text{Fe}_2\text{O}_3$ ,  $\text{CuO}$ , and  $\text{Pt}$  appeared to be attractive for our proposed conditions of  $\sim 5$  atm and 1050 K. We assume that the G.A.  $\text{Fe}_2\text{O}_3$  catalyst is superior to Ispra's  $\text{Fe}_2\text{O}_3$  catalyst. Some GA data are plotted on the Ispra Fig. 3.13.

We have selected 0.5 s as the residence time for the  $\text{SO}_3$  decomposer as being safely on the high, flat portion of the conversion-residence time plot based on G.A.'s work. We have reviewed carefully the G.A. work at 1050 K and found that we could eliminate the expensive platinum catalysts by substituting the much cheaper  $\text{CuO}$  or  $\text{Fe}_2\text{O}_3$  catalysts. These latter catalysts perform nearly identically; however, they are both deactivated by a sulfation reaction involving the substrate on which the active metal oxide is placed. We have selected  $\text{CuO}$  as preferable on the basis of a deactivation temperature around 950 K, as compared to  $\text{Fe}_2\text{O}_3$  at 1000 K.

Packing information and the definition of the residence time,  $t$ , used by G.A. was used to estimate the catalyst requirements for a fluidized bed decomposer. The decomposer maximum total volumetric flow (including  $\text{H}_2\text{O}$ ,  $\text{SO}_3$  and recycle) for our plant when driven by a 5,000 Mwt TMR with a process heat demand of 608.85 kJ/gmol  $\text{H}_2$  was calculated to be 437  $\text{m}^3/\text{s}$  at 1050 K and 6.5 atm. The latter pressure was selected as an average of the  $\text{SO}_3$  decomposer inlet and outlet conditions. We estimated the volume of required catalyst to be 560  $\text{m}^3$ , assuming the same catalyst geometry as was used in the experimental work of G.A.

### 3.12.4 A Fluidized Bed SO<sub>2</sub> Decomposer Design

The design of chemical reactors with fast kinetics and large associated heat effects is one of the toughest problems in the chemical process industries. We spent a substantial effort examining different types of chemical reactors to try to establish a design of least cost and greatest simplicity.

The analysis for a plug-flow, packed bed reactor shows this not to be practical because of large temperature gradients (i.e., 68 °C) between the heat exchanger fluid supplying the heat and the packed bed.

This problem has led us to fluidized bed designs. Using a catalyst particle size of 0.5 mm the minimum fluidization velocity,  $U_{mf}$ , we estimated as  $U_{mf} = 0.0428$  m/s. This velocity is well below the entrainment velocity,  $U_t = 3.67$  m/s. We have selected the velocity to be  $U_f = 1$  m/s. At this velocity, we estimated the bed expansion to be  $\epsilon = 0.8$ . Consequently, the new bed volume was 1627 m<sup>3</sup> total, which we divided up into seven units of reasonable but large size: 8 m high by 6 m in diameter. The fluidized bed catalytic SO<sub>2</sub> decomposer is illustrated in Fig. 3.14.

For such decomposer vessels, we estimated a  $P = 1.66$  atm. We also allowed about 1 atm pressure drop across the distributor plate; thus  $P = 2.6$  atm total. The pumping work for fluidizing the seven units would be 51.4 MW<sub>e</sub>. This work requirement is for 6.3 kJ/gmol H<sub>2</sub> per unit H<sub>2</sub> production. We consider this to be an attractively small value.

#### Varying the Decomposer Temperature

A parametric study was done on varying the decomposer temperature. The mass balances were done for 100 K higher and 100 K lower temperature than the 1050 K reference. The flow vessel

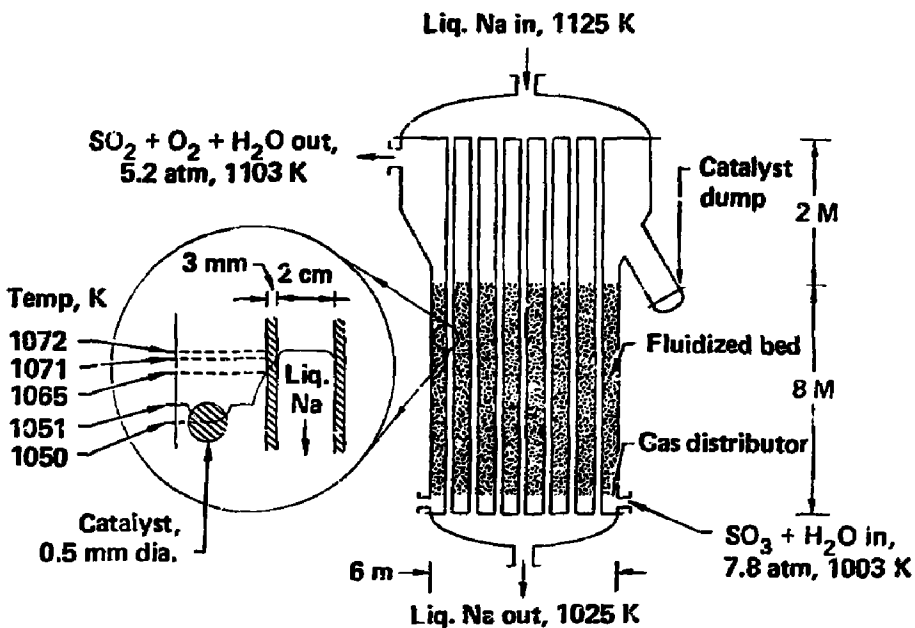


Fig. 3.14 Fluidized Bed Catalytic SO<sub>3</sub> Decomposer

sizes and costs and pumping power are shown in Table 3.5. There is a clear tradeoff between lower temperature and increased evaporator and decomposer vessel size, pumping power, and costs.

TABLE 3.5  
A PARAMETRIC STUDY ON VARYING DECOMPOSER TEMPERATURE

	DECOMPOSER TEMPERATURE		
	1144 K	1050 K	950 K
SO <sub>3</sub> Conversion, SO <sub>3</sub> SO <sub>2</sub>	0.735	0.55	0.29
Total Molar Flow in Evaporators, gmols/s	27,530	35,560	61,292
Volumetric Flow in Evaporators, m <sup>3</sup> /s	397	437	735
Volume Decomposer Catalyst, m	466	560	942
Number of Catalytic Decomposers in Use	6	7	12
Fluidization Pumping Power, kJ/gmol H <sub>2</sub>	5.5	6.3	10.9
Liquid Sodium Pumping Power, kJ/gmol H <sub>2</sub>	2.5	2.9	5.0
Approximate Decomposer Installed Costs Incoloy-800, M\$	45	50	90

The choice of material for a sodium-driven SO<sub>3</sub> decomposer would involve, on the sodium side, a 0.5 mm steel clad (Fe, 2-1/4% Cr, 1% Mo) on the inside of the Incoloy 800H heat exchanger tubes. On the SO<sub>3</sub> process side, the Incoloy 800H would be coated with an aluminide layer, 100 μm or so thick.

#### Helium as an Increased Safety Option

We repeated the design procedure, replacing the liquid sodium by helium as the heat transfer medium to carry the blanket heat out to the H<sub>2</sub> thermochemical plant. We used a ΔT = 50 °C across

the  $\text{SO}_3$  decomposer and operated helium at 30 atm total pressure in order to minimize the stresses on the  $\text{SO}_3$  decomposer internal tubes. The helium mass flow required was 1200 kg/s per bed or 120 m/s velocity for a decomposer with 18,000 tubes per bed (twice the number and twice the cost as in the sodium unit). The film  $\Delta T$  for helium to the inside of these tubes was 18  $^\circ\text{C}$ , thus raising the overall  $\Delta T$  to about 30  $^\circ\text{C}$ , very little above the sodium unit's 22  $^\circ\text{C}$ . The pressure drop was 1.0 atm across the decomposer, creating a pumping power of 8.1 kJ/gmol  $\text{H}_2$  for all seven beds. Thus, from the decomposer standpoint, He is a viable candidate and achieves greatly improved safety isolation. High helium pressures (i.e., 60 atm) would allow reducing the number of tubes back to 9,000, and reduce pumping power; but the added pressure would force us to double the tube thickness from 3 mm to about 6 mm. The materials we have selected for the He-driven  $\text{SO}_3$  decomposer would involve IncoIoy-800H at 2 mm thick wall, 20 mm diameter O.D., under our conditions of 30 atm. The stress level would be around 7.15 MPa (1100 psi).

### 3.13 Process Chemistry Structural Materials

In interfacing the Cauldron blanket design with the G.A. Sulfur-Iodine Cycle, our most critical materials needs involve the following components:

- Transport piping
- Heat exchanger -  $\text{SO}_3$  decomposer
- Heat exchanger -  $\text{H}_2\text{SO}_4$  boiler

Materials requirements for these components involve considerations of corrosion resistance, good creep strength, low cost, and ease of fabrication.

For the transport piping between the Cauldron and the  $\text{SO}_3$  decomposer, we have selected the alloys In-800 and In-800H as best meeting the various materials needs when either liquid Na or potassium is used for heat transport. Corrosion is of dominant concern here, and temperatures have to be maintained at  $\sim 1100$  K or less in order to provide adequate lifetimes. If high pressure helium is used as the heat transport fluid, corrosion is no longer a problem, but long-term creep strength becomes of major concern. The alloys In-800 (or In-800H), In-617, and In-625 are selected for use with helium, with In-617 having the best creep strength ( $\sim 3600$  psi for 1% creep in 100,000h at 1150 K).

The  $\text{SO}_3$  decomposer requires the highest process temperature input of the G.A. Sulfur-Iodine Cycle at  $\sim 1100$  K. On the heat delivery side of the process heat exchanger (which is envisioned to have tubes 2 cm in diameter and 2-3 mm wall thickness), creep is the main problem. On the chemical process side, corrosion by decomposing  $\text{SO}_3$  gas is of major concern. In view of the experiences gained at Ispra and at the General Atomic Company, we select In-800H, that has been coated with aluminide on the process side, as the heat exchanger alloy. Lifetime is expected to be of the order of 20 years.

The heat exchanger for the  $\text{H}_2\text{SO}_4$  boiler presents the most critical corrosion problem in the G.A. Sulfur-Iodine Cycle. The boiling is carried out at  $\sim 673$  K and 10 atm pressure for the water- $\text{H}_2\text{SO}_4$  azeotrope (equivalent liquid and vapor compositions) that occurs at 97 wt %  $\text{H}_2\text{SO}_4$ . Ordinary metallic materials are severely corroded under these conditions. A ceramic heat exchanger made of siliconized SiC (a 2-phase mixture of SiC and Si) offers us the best prospect for this component. Such heat exchangers have only been made in a developmental mode, but show attributes such as: being impervious to gases, high thermal conductivity, high strength, good thermal shock resistance, excellent corrosion resistance,

and they can be fabricated in complex shapes and bonded together to form heat exchanger assemblies. In spite of the developmental nature of a siliconized SiC heat exchanger, we select it as our best choice.

The best commercial material available for the  $H_2SO_4$  boiler is Durichlor-51, which is a high silicon cast iron intermetallic with an approximate composition of  $Fe_3Si$ . Considerable care needs to be exercised in the manufacture and fabrication of this material because of porosity in the structure and poor ductility. We estimate a lifetime of the order of 5y for Durichlor-51 in this application. Yet another prospective developmental material for the  $H_2SO_4$  boiler is  $CrSi_2$  coated In-800.

### 3.14 Coupling the Fusion Reactor to the Thermochemical Hydrogen Production Process

The objective of this present study was to assess the feasibility of producing hydrogen by utilizing a Tandem Mirror Reactor (TMR) and one of three promising thermochemical or thermo-electro-chemical cycles. The complete system consists of four sub-systems as illustrated in Fig. 3.15. The energy conversion and transport system couples the fusion reactor to the thermochemical plant. This subsystem consists of the heat exchangers and coolants required to transport thermal energy from the fusion reactor blanket to the thermochemical process. It also includes the energy conversion equipment, associated thermodynamic cycle, and working fluids utilized to convert thermal energy into mechanical work or electricity.

Of the three cycles reviewed, the G.A. Sulfur Cycle was selected for preliminary evaluation of: (a) the various options available for coupling a fusion reactor to these types of cycles; and (b) the problems associated with each option. The

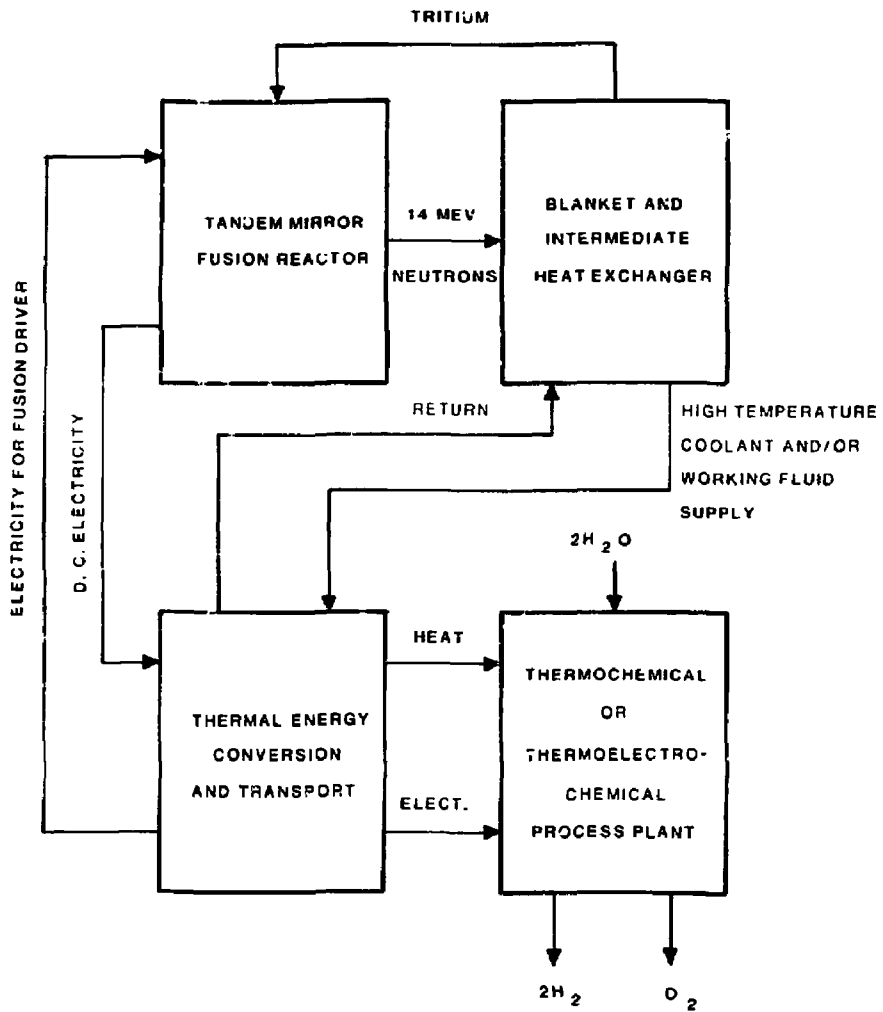
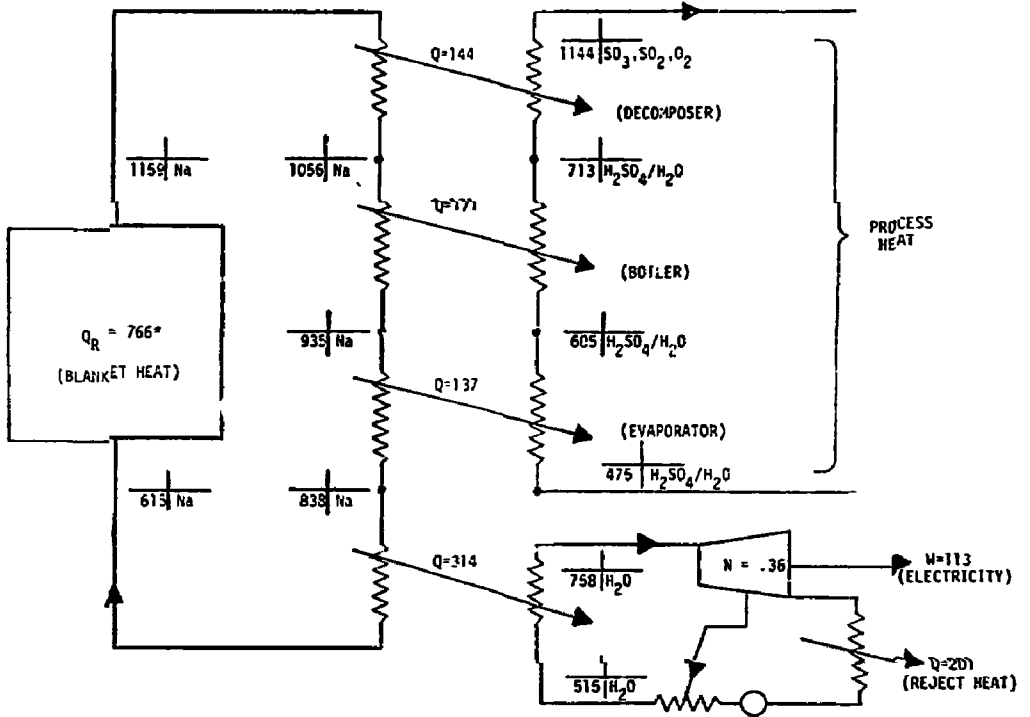


Fig. 3.15 Fusion-based hydrogen production system

thermal and work (or electrical) input requirements for the three different cycles are similar in many respects. Although the utilization of these energy forms within the different cycles differs significantly in some cases, the energy conversion and transport systems could possibly be quite similar.

The primary results of this aspect of the study are summarized below.

- (a) From a system arrangement standpoint, the simplest means for meeting the energy conversion and transport needs of the G.A. thermochemical cycle as developed by G.A., utilizing state-of-the-art equipment as much as possible, is through the use of a single sodium transport loop between the fusion reactor blanket (either  $\text{Li}_2\text{O}$  or  $\text{Li/Na}$ ) and the thermochemical cycle. Process heat exchangers and a steam generator are arranged in series. Process heat would be transferred from the high temperature portion of the loop, and a bottoming steam cycle operating at conditions typical of LMFBR technology would utilize the lower temperature energy for generating electricity. The sodium loop would isolate the thermochemical cycle from activation products and tritium. The concept is illustrated in Fig. 3.16.
- (b) The two basic energy requirements are for process heat and shaft work or electricity. The fractional division of energy together with the four primary heat exchangers required follow:



\*Heat and Work Units -  $\frac{kJ}{.993 \text{ g-moles } H_2}$

$$n = \frac{285}{766} = .37$$

$\frac{MPa}{^{\circ}K} \frac{\text{mass}}{\text{Time}^2}$   
Fluid

Fig. 3.16 Single series Na loop - electric power generation based on LMFBF technology - subsystem A

Heat Exchanger	% Heat	Process Media	Sodium Temp.		Process Temp.	
			High	Low	High	Low
Decomposer	19	SO <sub>3</sub> , SO <sub>2</sub> , O <sub>2</sub>	1159 K	1056 K	1144 K	713 K
Boiler	22	H <sub>2</sub> SO <sub>4</sub> , H <sub>2</sub> O	1056	935	713	685
Evaporator	18	H <sub>2</sub> SO <sub>4</sub> , H <sub>2</sub> O	935	838	685	475
LMFBR Type Steam Generator	41	Steam for Electricity Generation	838	615	758	515

- (c) Limitations in the technology base center around the blanket design, the intermediate heat exchanger (Li<sub>2</sub>O/Na or Na/Na), the transport of sodium between the intermediate heat exchanger and the process, and subsequently the transport of heat from the sodium to the process streams.

The combination of temperatures and fluids involved requires a new assessment of available materials for piping and heat exchangers in terms of their mechanical properties and chemical compatibility. Possibly the development of new materials will be required. Clearly no similar commercial state-of-the-art application exists; however, there has been some work done for the space program and recent reviews for the fossil energy program on the operation of alkali metal vapor cycles for generating power at similar operating temperatures, which may be applicable to some extent.

- (d) Transport and conversion systems based on the use of helium, or potassium (vapor and liquid), are possibilities for coupling the TMR to the GA thermochemical cycle. Both of these options appear to be capable of higher efficiency than the simple series sodium loop option. The helium option has a technology base stemming from high temperature gas cooled reactors (HTGR's). However, high pressures

(50-70 atmospheres) and high parasitic pumping power requirements would have to be dealt with in both the blanket and transport and conversion system. The technology base for potassium appears to be less developed than for either sodium or helium. Potassium system pressures at vapor locations would be 4-5 atmospheres. This is significantly lower than the helium option, but also significantly higher than an atmospheric pressure sodium system. Potential helium and potassium based systems are illustrated in Figs. 3.17 and 3.18, respectively.

- (e) The high temperatures at which process heat from the fusion reactor is required can be significantly reduced from that required by the cycle developed by GA by a simple modification. The modification involves recycling part of the hydrogen product stream and utilizing the heat of oxidation in the decomposer. The hydrogen could be combusted external to the decomposer heat exchanger or oxidized in situ in a reaction vessel.

There is a significant reduction in overall efficiency as a result of hydrogen recycle--on the other hand, it significantly reduces the temperature/materials issues associated with (a) the blanket, (b) the transport of the thermal energy from the blanket to the thermochemical process, and (c) the heat exchanger between the reactor coolant and the high temperature process media.

- (f) System efficiencies can vary widely (from 27 to 48%) for the options evaluated depending on the approach utilized (see Table 3.6). Since there is no input of feedstocks to the combined fusion/hydrogen plant, plant efficiency is only important in terms of its indirect effect on hydrogen production costs which does not necessarily imply maximizing efficiency is the criterion upon which this plant system should be based. Attempting to obtain very

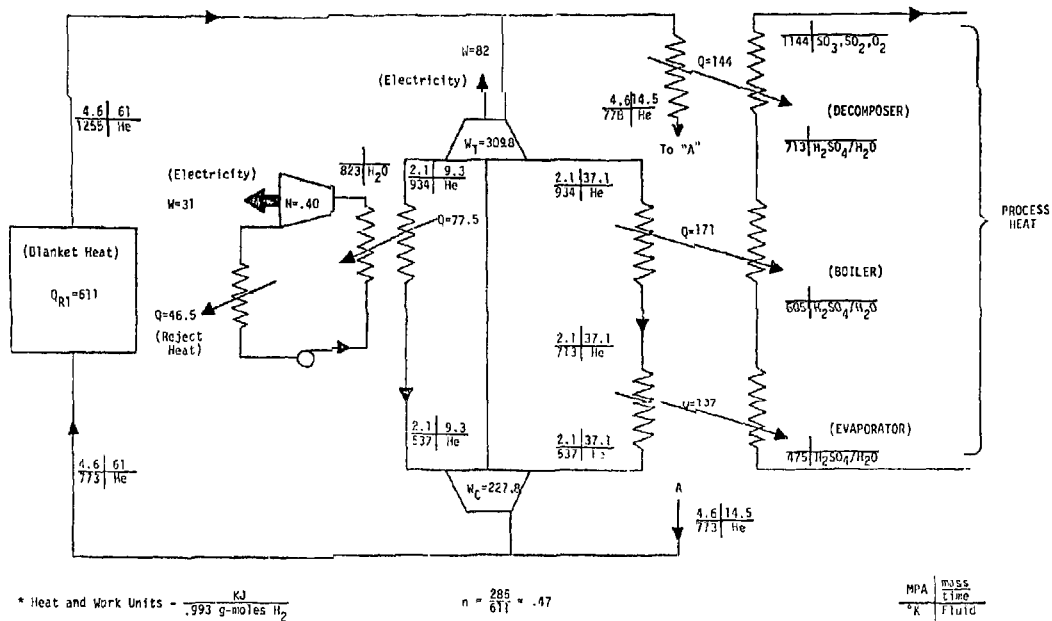


Fig. 3.17 Combined series/parallel subsystem utilizing He as the thermal transport media and working fluid for generating most of the required electricity - subsystem B

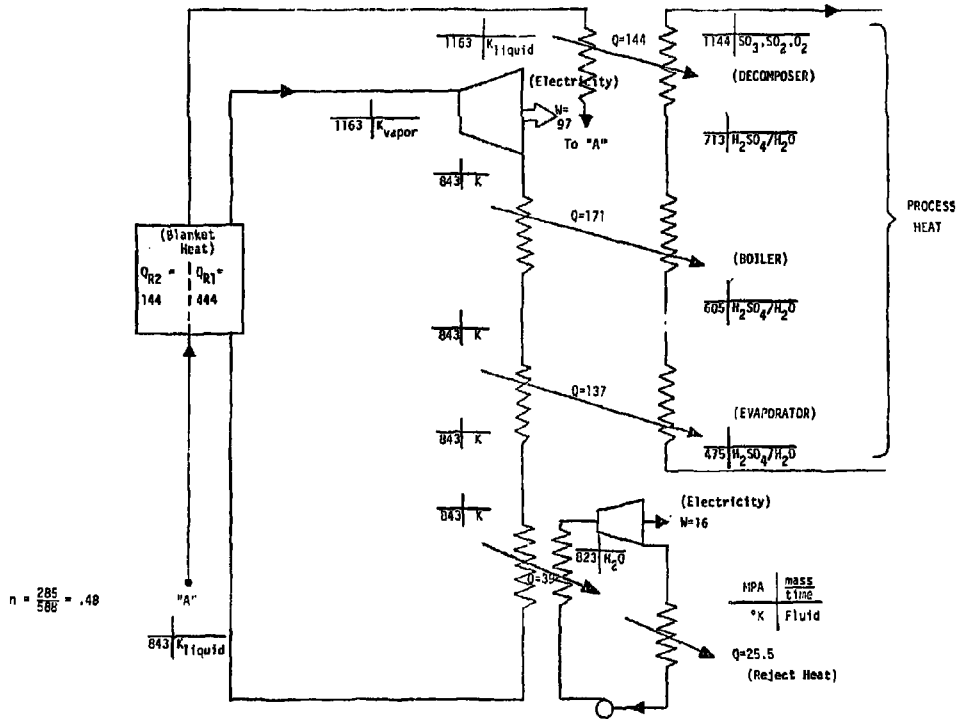


Fig. 3.18 Combined series/parallel subsystem utilizing K as the working fluid

TABLE 3.6

COMPARISON OF CONVERSION AND TRANSPORT OPTIONS

<u>Options</u>	<u>Maximum TMR Blanket Outlet Temperature Considered</u>	<u>Efficiency %</u>	<u>Remarks</u>
A. Single Series Sodium	1159 K	37	Underdeveloped at High Temperature, Technology Base Below 800 K
B. Helium Series/ Parallel	1255 K	46	High Pressure, High Pumping Power, Technology Under Development
C. K Series/Parallel	1163 K	48	Limited Technology Base
D. K Parallel	1163 K	43	Limited Technology Base
E. Sodium With Hydrogen Recycle	838 K	27	Least Technological Development Required

high efficiency utilizing extremely high temperatures may result in high material costs, excessive down time, and higher production costs than the economic optimum. Clearly an optimization of production costs is beyond the scope of this preliminary assessment; however, it must be the basic criterion for any meaningful plant engineering design study conducted beyond this preliminary technological assessment.

### 3.15 Integrated TMR - Synfuel Plant Energy Balance

As discussed in Section 3.4, the primary use of the thermal power generated by the Tandem Mirror Reactor is for the synthesis of hydrogen gas. However, a portion of this power must be distributed to various plant facilities in the form of electricity. In Figs. 3.19 and 3.20 we show power flow diagrams for the overall system consisting of the TMR, its blanket and direct converter, the power distribution system and the synfuel plant. In Fig. 3.19 the power distribution system is taken to be the single series Na loop of Fig. 3.16, and the TMR blanket has the characteristics of the baffled  $\text{Li}_2\text{O}$  blanket. In Fig. 3.20 the power distribution system corresponds to the combined series-parallel system of Fig. 3.18 with a potassium-vapor topping turbine whose thermoelectric efficiency is  $\eta_T = 0.20$ . The ratio of electrical and thermal powers of the synfuel plant (600 MWe/2641 MWe) is the same as the ratio of the total work plus electricity and thermal input per g-mole  $\text{H}_2$  (113 KJ/452 KJ).

In Figs. 3.19 and 3.20 are shown the fusion, thermal and electric processes corresponding to a synfuel plant output of  $1671 \text{ MMH}_2$  ( $1.13 \times 10^{10}$  liter/day). For the particular cases shown the gain  $Q = P_{\text{FUS}}/P_{\text{in}}$  ( $= 11.6$ ) has been adjusted so that the external recirculating power  $P_{\text{RC}}$  is zero.

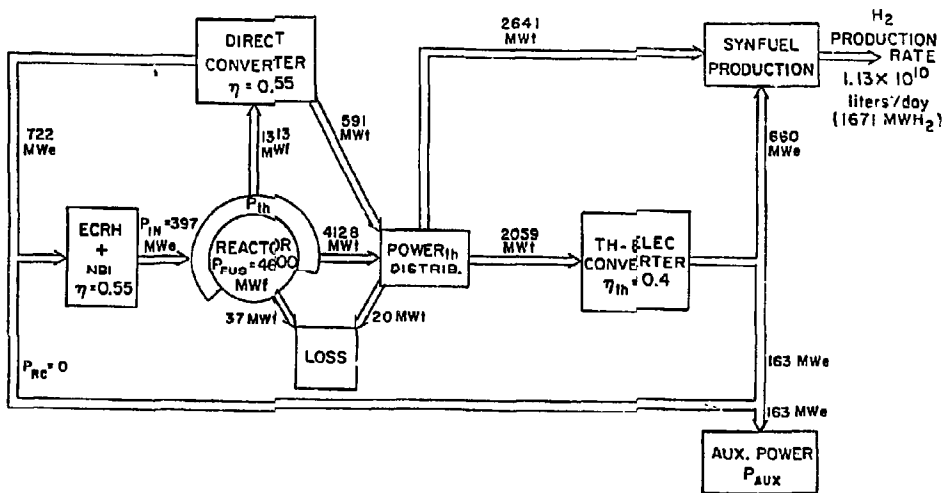


Fig. 3.19 Power flow diagram for the TMR-synfuel system with peotting electric power generation. For the case shown  $Q = 11.6$ .

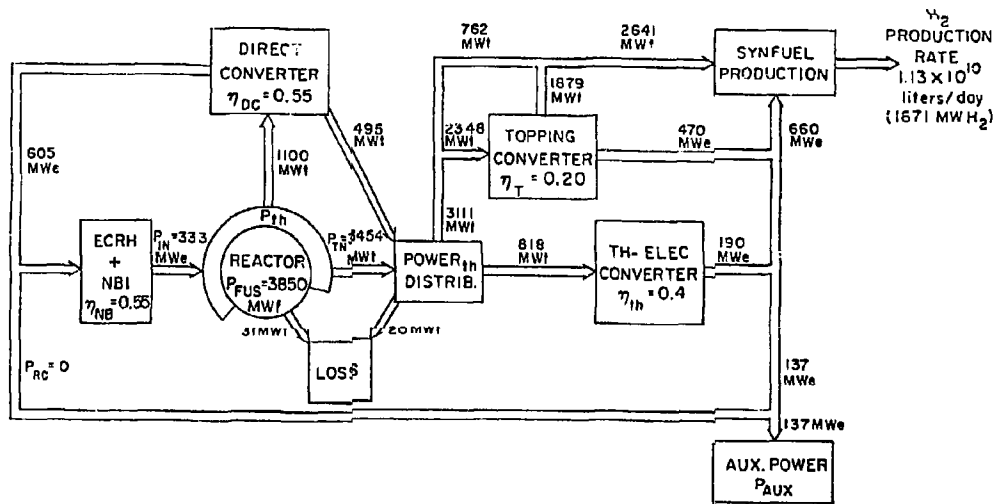


Fig. 3.20 Power flow diagram for the TMR-synfuel system with topping and bottoming electric power generation. For the case shown  $Q = 11.6$ .

Figure 3.21 shows  $P_{FUS}$  and  $P_{RC}$  as functions of  $Q$  for a fixed synfuel plant output of  $1671 \text{ MW}_{H_2}$ . For  $Q = 11.6$ ,  $P_{FUS} = 4600 \text{ MWf}$  and  $3850 \text{ MWf}$  for the bottoming and topping cases, respectively. The topping case corresponds to the TMR parameters listed in Table 3.1. The overall thermal efficiency  $\eta = P_{H_2}/P_{FUS}$  is 0.36 and 0.43 for the two cases. The efficiencies of converting blanket thermal energy to hydrogen chemical energy are 0.39 and 0.47, comparable to the values 0.37 and 0.48 given in Figs. 3.16 and 3.18.

In Fig. 3.21, the arrows on the right indicate the limiting values of  $P_{FUS}$  and  $P_{RC}$  as reactor gain  $Q$  (or length) becomes very large. For both the topping and bottoming cycles  $P_{RC}(\alpha)/P_{FUS}(\alpha) = 0.11$ . This corresponds to the limit  $[P_{DC} - (P_{AUX} - P_{CIRC})]/P_{NET} = 0.12$  shown in Fig. 3.16.

### 3.16 Looking to the Future - The IMR and the DD or D-He<sub>3</sub> Cycle

When we consider only the D-T fuel cycle, there is a limit for the charged particle energy out of the TMR that cannot exceed 20% of the total energy output, i.e., 3.5 Mev alphas (14.1 Mev neutrons + 3.5 Mev alphas).

If a D-D fuel cycle were to be considered the picture changes significantly. With the D-D cycle, it is possible to have approximately 50% of the raw energy output of the TMR in charged particle form and convertible to electricity directly. It is interesting to compare the two cycles (the DT and the DD) for their overall plant efficiency potential and also to compare the TMR with the tokamak, the HTGR or a solar concentrator under these circumstances. This comparison is shown in Fig. 3.22.

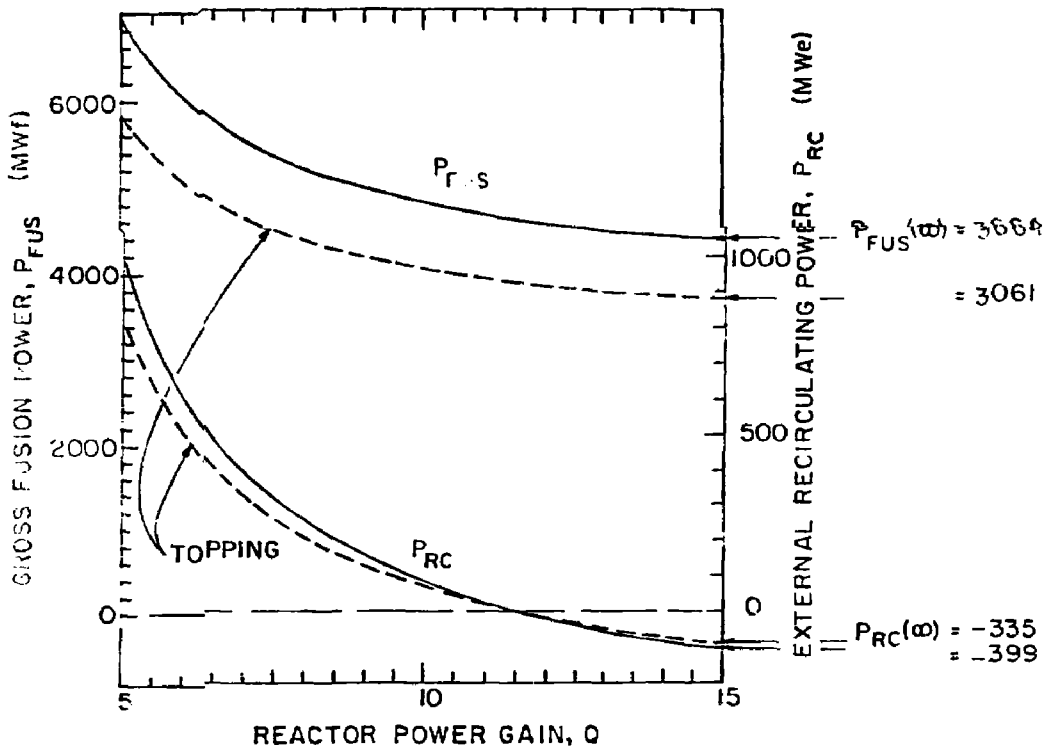


Fig. 3-21 Gross fusion power and external recirculating power as functions of fusion reactor gain  $Q$

o Tandem D-T Cycle

$$\eta_{\text{net}} = 0.8 \eta_{\text{th}} + 0.2 \left[ \eta_{\text{dc}} + (1 - \eta_{\text{dc}}) \eta_{\text{th}} \right]$$

$$\eta_{\text{net}} \approx 0.32 + 0.146 \approx 47\%$$

o Tandem D-D Cycle

$$\eta_{\text{net}} = 0.5 \eta_{\text{th}} + 0.5 \left[ \eta_{\text{dc}} + (1 - \eta_{\text{dc}}) \eta_{\text{th}} \right]$$

$$\eta_{\text{net}} \approx 0.20 + 0.365 \approx 57.5\%$$

o Tokamak D-T Cycle or D-D Cycle, the HTGR or a Solar Concentrator

$$\eta_{\text{net}} = \eta_{\text{th}}$$

$$\eta_{\text{net}} = 0.40 \approx 40\%$$

Fig. 3.22 Overall Efficiency Potential of Different Energy Sources

We are of the opinion that the D-D cycle, although difficult from a physics standpoint, may be significantly superior to D-T from an engineering/technology viewpoint. The economics may be in question because of poorer reaction cross-section. However, the environmental/political influences and pressures that will inevitably be brought to bear on fusion's acceptability to the community cannot be ignored. The inexhaustible energy advantages and safety advantages of deuterium fuel over tritium fuel are also important and particularly interesting when coupled to the production of hydrogen.